UNIVERSITY OF BIRMINGHAM

Low Dose Demethylating Agents in Oral Cancer

and

The Respiratory Phenotype of *Phd1*$^{-/-}$ Mouse Liver Mitochondria

Hannah Jessica Eadie

This project is submitted in partial fulfilment of the requirements for the award of the MRes.

College of Medicine and Dentistry

University of Birmingham

May 2014

Table of Contents- Project 1

Table of Contents- Project 2

List of Figures- Project 1

Tables-Project 1

List of Figures- Projec2

Tables –Project 2:

UNIVERSITY OF BIRMINGHAM

COLLEGE OF MEDICINE AND DENTISTRY

PROJECT 1

Low Dose Demethylating Agents In Oral Cancer

Hannah Jessica Eadie

Supervisors: Dr M. Wiench, Dr B. Scheven

and Prof. P. Cooper

May 2014

This project is submitted in partial fulfilment of the requirements for the award of the MRes.

Abstract

DNA methylation is a gene silencing mechanism. In cancer the normal pattern of DNA methylation is often disrupted; silencing tumour suppressor genes and leading to uncontrolled progression through the cell cycle. Therefore DNA demethylating agents represent a promising therapeutic pathway to pursue. While 5-Aza-2'deoxycytidine (DAC) is a demethylating agent approved by the FDA for the treatment of myelodysplastic syndromes (MDS) and its use thus far has been confined to haematological malignancies, current research suggests treatment may be transferable to solid tumours. Progress in this area has been hindered by toxicity at higher doses however low doses of DAC may provide the benefits of DNA demethylation without the toxic side effects. In this project I examined the effect of various concentrations of DAC on two oral cancer cell lines; Vu40T and Scc040. Data indicated that a concentration as low as 100nM DAC was sufficient to reactivate the tumour suppressor gene RARβ in Vu40T cells. However this result is specific as it differed between the cell lines and culture method used. Furthermore DAC treatment lead to an increase in 5-hydroxymethycytosine (5hmC) levels in both cell lines and a corresponding increase in TET2 gene expression suggesting that DAC reactivates TET2 which then converts 5mC to 5hmC. These results suggest that the benefits of low dose DAC may be transferable to the treatment of solid tumours and provides two potential mechanisms by which it exhorts its effects in oral cancer.

Introduction

Oral Cancer

Oral cancer is becoming a major health problem with the World Health Organization predicting an increase in cases for decades to come (Sciubba, 2001). The term covers cancers of the oral cavity, oropharynx and lip vermilion with the vast majority of cases being oral squamous cell carcinomas (OSCC) which arise from the oral mucosal lining (Neville and Day, 2002). As with all cancers OSCC is a multifactorial disease and excessive tobacco or alcohol consumption and HPV infection contribute to increased risk (Gasche and Goel, 2012). What is of increasing interest in oral cancer research is the dysregulation of gene expression via epigenetic modifications (Gasche and Goel, 2012).

DNA Methylation

This project studies one aspect of epigenetics specifically: DNA methylation. DNA methylation is the addition of a methyl group to a DNA base, usually position five of the pyrimidine ring of cytosine in CpG dinucleotides, a reaction catalysed by the DNA methyl transferases (DNMTs) (Gasche and Goel, 2012). The modification is associated with gene silencing via Methyl-CpG-binding proteins (MBPs) which liaise with co-repressors to bring about a closed chromatin state (Klose and Bird, 2006). CpG sequences are underrepresented in the genome and the majority are methylated. The exception is CpG islands which are regions rich in CpGs usually found near gene promoters (Tsai and Baylin, 2011). 85-90% of these sites are left unmethylated in any given cell allowing the associated genes to be transcriptionally expressed (Tsai and Baylin, 2011). However in many cancers this

normal pattern of methylation is disrupted and the abnormal methylation of tumour suppressor genes can lead to uncontrolled progression through the cell cycle suggesting that demethylating agents may provide a promising therapeutic pathway to pursue (Tsai and Baylin, 2011).

In a methylation array of 44 OSCC patient samples Jithesh et al. (2013) found that OSCC has a methylation profile distinct from that of healthy tissue with the majority of probes examined being hypermethylated in the OSCC samples. A similar result was found by Jäwert et al. (2013) who used immunohistochemical analysis to compare oral mucosal samples from healthy patients to those with OSCC and found the methylation levels in OSCCs were significantly higher. Additionally multiple genes known to be associated with tumour suppression are found to be hypermethylated in oral cancers including APC, $p14^{ARF}$, E-Cadherin and RARβ with this silencing contributing to tumour progression (Gasche and Goel, 2012).

DNA Hydroxymethylation

DNA methylation is reversible and this is known to be an active process in certain situations however exactly how it is regulated is unclear. The discovery that 5-methylcytosine (5mC) can be oxidised to form 5-hydroxymethylcytosine (5hmC) which can then be converted to 5-formylcytosine (5fC) and finally to 5-carboxylcytosine (5caC) has provided a potential mechanism for DNA demethylation as 5caC can be converted back to cytosine in either an active or a passive process (Tahiliani et al., 2009; Ito et al., 2011; He et al., 2011; Piccolo and

Fisher, 2014). This reaction is catalysed by the TET protein family (1, 2, 3) of Fe^{2+} and α- ketoglutarate (α-KG) dependent dioxygenases (Ito et al., 2011).

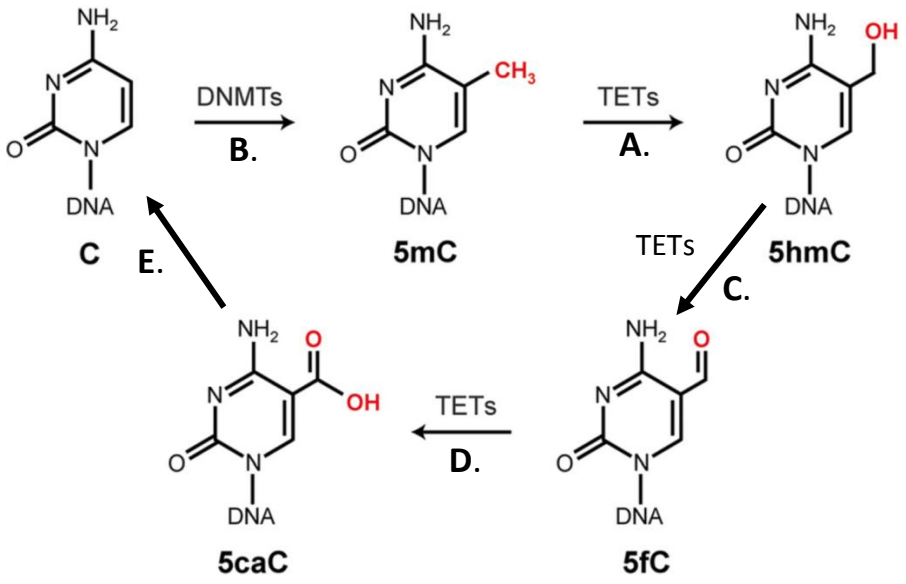

Figure 1: DNA Demethylation Pathway. A: *DNMTs catalyse the addition of a methyl group to position 5 of the pyrimidine ring of cytosine.* ***B:*** *TETs hydroxylate 5mC into 5hmC.* ***C-D:*** *5hmC can be further oxidised into 5fC and 5caC if ATP is supplied.* ***E:*** *5caC can be removed by thymine DNA glycosylase (TDG) and replaced with C or lost during DNA replication when the modification is not passed on to the daughter stand of DNA. Image adapted from Tan and Shi, (2012).*

In addition to analysing the methylation status of oral mucosal samples Jäwert et al. (2013) determined the levels of hydroxymethylation and the TET2 protein. They identified a decrease in 5hmC in the cancerous samples compared with healthy oral epithelium. This corresponded with a decrease in TET2 providing a mechanism to account for this loss (Jäwert et al, 2013). Similarly Yang et al. (2013) demonstrated using dot blot and immunohistochemical analysis that the 5hmC levels in various other organs were much lower in cancerous tissue compared with healthy tissue in both mice and humans. They also demonstrated via quantitative PCR (qPCR) that the expression of all three TET genes was lower in cancerous tissue compared with the corresponding healthy tissue for breast carcinoma and hepatocellular carcinoma thus providing a potential mechanism to explain the loss of 5hmC (Yang et al., 2013). These results are in agreement with

the theory that 5hmC is a step in the demethylation pathway and also suggests that 5hmC and the TET genes may have tumour suppressive functions.

5-Aza-2'-Deoxycytidine

Azacytidine (AZA) and 5-Aza-2'-deoxycytidine (DAC) are two demethylating agents that have proved effective in the treatment of haematological malignancies and as such are FDA (The US Food and Drug Administration) approved (Tsai et al., 2012). Both drugs are analogues of cytosine and are incorporated into DNA at cytosine sites. The use of these drugs has been limited by the fact that high doses are extremely cytotoxic however at low doses the positive effects of DNA demethylation may outweigh the negatives of DNA damage (Tsai et al. 2012).

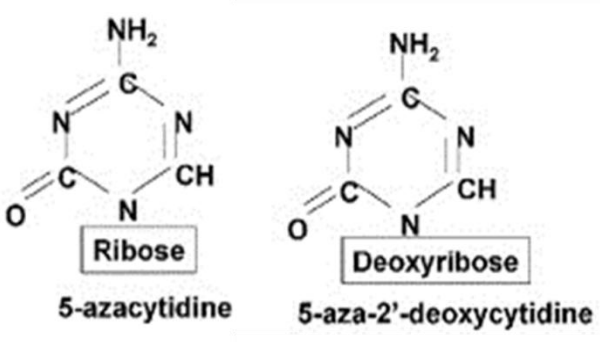

Figure 2: 5-Azacytidine (AZA) and 5-Aza-2'-deoxycytidine (DAC) are cytosine analogues. *Figure adapted from Leone et al. (2003).*

DNMT1 only methylates hemimethylated DNA; it copies DNA methylation onto the daughter strand after DNA replication making methylation heritable across cellular generations (Ghoshal et al., 2005). Both DNMT3a and DNMT3b are *de novo* methyl transferases (Gasche and Goel, 2012). Ghoshal et al (2005) found that the expression profile in DNMT1 knockout cells was similar to that of cells which had been treated with DAC. However, DNMT3b knockouts did not show the same pattern suggesting that DAC exerts its effects mainly through DNMT1. When DAC is incorporated into DNA in place of cytosine, DNMT1 recognizes and binds covalently to the base (Stresemann and Lyko, 2008). When DNMT1 is bound to

cytosine this bond is rapidly removed however the binding of DAC is more stable and hence it becomes trapped on DNA (Stresemann and Lyko, 2008). This is thought to lead to the cytotoxic effects of DAC as it can cause DNA damage and notably when DNMT1 is reduced the toxicity of DAC is also reduced (Jüttermann et al., 1994). DNMT1 is then selectively degraded by the proteasomal pathway hence DAC treatment leads to a decrease in available DNMT1 and a corresponding decrease in methylation (Ghoshal et al., 2005). As such the levels of DNMT1 in the cells contribute to the efficacy of the drug and may explain why some cancers are resistant to treatment.

5-Aza-2'-deoxycytidine was recently shown to have therapeutic benefits against myelodysplastic syndrome (MDS) in a randomized phase III clinical trials which lead to its approval by the FDA (Kantarjian et al., 2006). Further success has been found in its use in the treatment of other haematological malignancies such as acute and chronic myeloid leukemia (AML and CML) (Leone et al., 2003; Issa et al., 2004). High doses of DAC are subject to toxicities due to the generation of DNA adducts caused by the capture of DNMT1 however it has been observed that low doses are just as effective (Issa et al., 2004). Tsai et al. (2012) showed that low dose DAC caused a decrease in promoter methylation, subsequent gene re-expression and the inhibition of subpopulations of cancerous cells not only in leukemic cells *in vitro* but also breast cancer cells demonstating that the benefits of low dose DAC may be transferable to solid tumours.

Retinoic Acid Receptors

Retinoic acid receptors (RARs) are nuclear receptors for retinoids and their derivatives (Connolly et al., 2013). Activation of the receptors can induce differentiation in various cell types and as such their inactivation has been noted in various malignancies (Connolly et al., 2013). There are three types of RAR (α, β, γ) which form heterodimers with RXRs (α, β, γ) and bind to RA response elements (RAREs) which are DNA sequences located 5' of RA induced genes (Connolly et al., 2013). In the absence of a ligand these associate with large protein complexes that bring about a condensed chromatin state (Duong and Rochette-Egly, 2011). However ligand binding induces a conformational change in the protein resulting in dissociation from co-repressors and the recruitment of co-activators leading to an open chromatin structure and transcription of associated genes (Duong and Rochette-Egly, 2011).

The expression of RARβ is dependent upon activation of RARα as RARβ is one of its downstream targets. However once active RARβ can regulate its own expression along with that of its target genes (Connolly et al., 2013). The genes regulated by RARβ are generally associated with cell differentiation and death hence RARβ is associated with tumour suppression and is commonly mutated or epigenetically silenced in solid tumours (Connolly et al., 2013). Low levels of RARβ expression are seen in premalignant oropharyngeal lesions indicating that gene activity is often lost early in tumourgenesis (Lotan et al., 1995). In most cases this loss of expression can be restored by treatment with retinoic acids however this is not always the case (Lotan et al., 1995). Epigenetic silencing of RARβ is thought to contribute to the lack of success of RAs in cancer treatment as

pharmacological doses of RA are not always sufficient to reactivate the gene, the repressive marks must also be removed. By using a combination of all-trans retinoic acid (ATRA), DNA methyltransferase inhibitors and histone deacetylase inhibitors Raffoux et al. (2010) had some success in the treatment of AML and MDS.

3D Cell Culture

Traditionally cancer cell lines have been grown in monolayers on culture-plasticware as this has provided a relatively easy to use system where various aspects of cell biology can be examined. However this is not an accurate model of how tumour cells behave *in vivo* and subsequently 3D systems have been developed to provide better *in vitro* representation (McCaffrey and Macara, 2011). These models allow for studies into morphogenesis and tumour invasion however they also show distinct differences in gene expression compared with 2D culture with the expression profiles of 3D cultured cells being more reminiscent of *in vivo* tumours compared with the same cells grown in monolayers (Ridky et al., 2010).

Aims and Objectives

This project aims to determine the effect of varying concentrations of 5'-Aza-2-deoxycytidine (DAC) on oral cancer cell lines either alone or in combination with 9-cis retinoic acid (RA). As relatively high doses have been shown to have harmful side effects the concentrations of DAC used in this project will range from 1μM to 10nM in order to determine the lowest concentration of DAC required to demethylated DNA. The efficacy of the treatment model will be assessed by determining changes in:

-RARβ gene expression;

-Local and global cytosine methylation levels;

-Global 5’ hydroxycytosine levels.

Two different oral cancer cell lines will be used to potentially replicate the diversity of *in vivo* tumours. Scc040 and Vu40T are both HPV-negative human oral cancer cell lines and despite their similarities, variation in the efficacy of the drugs on the two cell lines is likely.

Gene expression of a single cell line varies with the method of culture used; from 2D to 3D and even between the different methods of 3D culture (Ridky et al., 2010; Khan et al., 2012). Therefore an additional aim of this project is to determine whether growing and treating cells in 3D culture instead of traditional 2D monolayer has any effect on susceptibility to DAC. The 3D culture method used here involved seeding the cells onto a collagen raft embedded with fibroblasts. This construct is subsequently grown on the surface of the culture medium so that the liquid air interface is maintained. This approach gives the cells orientation and hence they differentiate into the different epithelial layers.

Materials and Methods

Cell Lines

Two HPV negative human oral cancer cell lines were used in this study; Scc040 (DSMZ) and Vu40T (a gift from Prof Hans Joenje, Free University of Amsterdam). Cultures were maintained in Dulbecco's Modified Eagles Medium (Sigma- Aldrich) supplemented with 10% fetal bovine serum, 5mg/ml penicillin-streptomycin (Gibco), 2mM L-glutamine, 0.1mM non-essential amino acids (Gibco) and 1mM sodium pyruvate (Gibco) in 37^{o}C and 5% CO_2.

Drug Treatments

For both cell lines 5x10^{4} cells were seeded onto a well of a 6 well plate for each treatment. This was performed in duplicate allowing one well for DNA extraction and one for RNA extraction. The drug treatments were performed over a 5 day period with the cells plated on day 1 and harvested on day 5 with the medium changed daily. 5-Aza-2'-deoxycytidine (DAC) was added to the medium on day 1 and 9-cis Retinoic Acid (RA) (Sigma-Aldrich Catalogue no: R4643) added on day 3 so that the cells were treated with 96 hours DAC and 48 hours RA. The cells were grown in 37^{o}C, 5% CO_2 in the dark as RA is sensitive to light.

For each cell line the following combinations of drugs were used: untreated control, 10nM DAC, 100nM DAC, 500nM DAC, 1µM DAC, 1µM RA, 10nM DAC + 1µM RA, 100nM DAC + 1µM RA, 500nM DAC + 1µM RA, 1µM DAC + 1µM RA. Two independent experiments were performed for Vu40T cells and three independent experiments for Scc040 cells.

DNA Extraction

Cultures were harvested for DNA extraction by washing in PBS solution (Sigma-Aldrich) twice, adding 750µl 0.25% trypsin (Gibco), allowing to trypsinize and inactivating with an equal volume of medium. The cells were then centrifuged for 5 minutes at 13000rpm to form a pellet, washed in cold PBS and stored at -20^{o}C.

DNA extraction was performed using the DNeasy Blood and Tissue kit (Qiagen) as of the blood and cell culture protocol. Briefly cells are first lysed with proteinase K and buffer AL then the DNA precipitated using 100% ethanol. The solution was then transferred to a spin column and centrifuged with a series of wash buffers to clean the DNA and remove ethanol from the sample. Once washed and dried the DNA was eluted in 200µl AE buffer and concentration determined using a NanoDrop.

Slot Blots

For each sample 1µg (or 500ng) of DNA was combined with 120µl 1M NaOH and 6µl 500nM EDTA up to a final volume of 300µl with dH_2O and a final concentration of 0.4M of NaOH. These were prepared in duplicate and heated at 100^{o}C for 10 minute to denature the DNA. The manifold was assembled with a sheet of filter paper under a sheet of nitrocellulose membrane both soaked in dH_2O for 10 minutes prior to assembly. The slot blot manifold was attached to a low level of suction and the wells washed with dH_2O. The heated samples were then added to the wells and allowed to pass through the slots onto the membrane. After all samples had passed through the slots 500µl 0.4M NaOH was added. The membrane was washed briefly in 2X SCC, allowed to dry and blocked for 1 hour

in 5% non-fat milk in dH_2O. The primary antibodies used were 5mC (Active Motif, Catalogue no. 39649) at a dilution of 1:1000 and 5hmC (Active Motif, catalogue no. 39769) at a dilution of 1:5000 both in 5% milk.

The primary antibodies were washed off in 5% milk, the secondary antibody added to the membranes (anti-mouse 1:5000 in 5% milk) and allowed to bind for 2 hours in 4^oC. This was then washed in PBS. The membranes were then treated with Amersham ECL western blotting detection reagents (GE Healthcare, catalogue no.RPN2106) for 1 minute before the slots were visualised.

ImageJ was used to determine the intensity of each band on the slot blots (Schneider et al., 2012). The results of each repeat were combined and density is shown relative to the band for the untreated control cells.

RNA Extraction, cDNA Synthesis and qPCR

RNA extraction was performed using the Qiagen RNeasy Mini kit as the protocol recommends. Briefly cultures were harvested by washing the wells twice in PBS solution (Sigma-Aldrich) then adding 500µl RLT buffer (Qiagen RNeasy kit) + 5µl β-mercaptoethanol. Following 5 minutes digestion the solution was homogenized using a 1mm needle and syringe and stored at -80^oC prior to use. Once defrosted 70% ethanol was added to homogenates; the solution transferred to an RNeasy spin column and the liquid removed by centrifugation for 15 seconds at 13000rpm. The spin column membrane was then washed in RW1 buffer and DNase added to digest any DNA contaminants. RPE buffer was added to the membrane and the spin column centrifuged at 13000rpm twice followed by a single 13000rpm

centrifugation in a clean collection tube to dry the membrane. Final RNA was eluted into 40µl nuclease free H_2O and a NanoDrop used to determine the concentration.

cDNA was synthesized using the iScript cDNA synthesis kit (Bio-Rad) from 1µg RNA and 0.1µl of reverse transcriptase. Using a thermal cycler the reaction mix was incubated at 25^{o}C for 5 minutes, 42^{o}C for 30 minutes then 85^{o}C for five minutes.

The Roche LightCycler 480 II qPCR system was used with 1µl cDNA, 0.075µl forward and 0.075µl reverse primers (all at 100mM), 6µl LightCycler 480 SYBR green master mix (Roche) and up to 12µl with dH_2O. The absolute quantification method was used with a standard curve generated from cDNA standards of known concentration. Each analysis was performed in duplicate.

qPCR Primers:

	Forward (5'-3')	**Reverse (3'-5')**
RARβ	TGCCAATACTGTCGACTCCA	CTCTGTGCATTCTTGCTTCG
RARα	GACCAGATCACCCTCCTCAA	CATCTGGGTCCGGTTCAG
GAPDH	CCTGGCCAAGGTCATCCAT	AGGGGCCATCCACAGTCTT
TET1	TCATGGGTGTCCAATTGCTA	GATGAGCACCACCATCACAG
TET2	GGACATGATCCAGGAAGAGC	CCCTCAACATGGTTGGTTCT
CK5	CCAAGCCAATTGCAGAACCA	AAATTTGGGATTGGGGTGGG
CK6	GTCCTCAGGCCCCTCTCTGG	CCCCTGGCAATTTTCTGCAA

qPCR Data Analysis

For each sample the concentration of RNA was determined from the number of cycles taken for it to cross the threshold fluorescent level (Crossing point, or Cp value). The concentration of the gene of interest for each sample was then normalised to the corresponding control gene (GAPDH or RARα). For each treated sample a fold change was generated against the untreated control cells. Each cDNA sample was analysed twice and a mean fold change was generated from all the biological and technical replicates for each sample and this is what is displayed in the figures. Microsoft excel was used to calculate standard deviations from the mean and these are shown as error bars. Excel was also used to perform the t-test on each sample against the untreated control cells to determine any significance in the findings: * = p-value<0.05, **= p-value<0.01, ***=p-value<0.005.

Bisulfite Conversion and Restriction Digest

Bisulfite conversion was performed using the Qiagen EpiTect Bisulfite conversion kit as the protocol recommends. In brief 500ng DNA was mixed with DNA protect buffer and bisulfite mix and conversion carried out in a thermal cycler (Program: 95^{o}C 5min, 60^{o}C 25min, 95^{o}C 5min, 60^{o}C 85min, 95^{o}C 5min, 60^{o}C 175min). Once complete the converted DNA was transferred to an EpiTect spin column and a series of buffers and centrifugation steps were used to clean the bisulfite converted DNA.

Primers were designed for RARβ transcription start site using the MethPrimer programme to generate primers specific to bisulfite converted DNA (RARβ Fwd:

AGAGGTAGGAGGGTTTATTTTTTGT, RARβ Rev: CAAATTCTCCTTCCAAATAAATACTTA) to generate a 182 base pair fragment. These were used to amplify the converted DNA using 2X Taq polymerase master mix (Thermo Scientific). Taqα1 restriction digest was then performed on 10µl of the PCR product using NEBuffer 4 (New England Biolabs), BSA (New England Biolabs) and 4 units of Taqα1 enzyme (New England Biolabs). These were incubated at 65^{o}C for one hour and inactivated at 85^{o}C for 20 minutes. The end products were electrophoresed on a 2% agarose gel in 0.75X TBE.

Raft Culture

3D organotypic raft culture was performed as previously described (Wilson et al., 2005) in collaboration with Dr Sally Roberts (School of Cancer Sciences, University of Birmingham). In brief Vu40T cells were seeded onto collagen rafts embedded with fibroblasts. The cells were cultured in Emedium (a gift from Dr Sally Roberts) supplemented with 10ng/ml epidermal growth factor (EGF) until fully confluent and then raised onto a metal grid. The grid was placed in a petri dish of Emedium without EGF with the medium touching the bottom of the grid and the top of the cells exposed to the air. Medium was changed every 48 hours and the cells cultured for 11 days with 100nM DAC added to the medium of one raft 4 days prior to harvest. The collagen was removed from the cells using a scalpel and each raft dissected into four equal sections, for RNA and DNA extraction purposes as described above.

Results

Sensitivity to DAC Varies Between Cell Lines.

In this study two oral cancer cell lines were studied, Scc040 and Vu40T. The cells were treated to four days of 5-Aza-2'-deoxycytidine (DAC) at varying concentrations with or without 9-cis retinoic acid (RA) for the final two days of culture. The effect of lower concentrations of DAC was of particular interest and the concentrations used were 10nM, 100nM, 500nM and 1μM DAC. Notably Tsai et al. (2012) classified very low doses as being in the range of 20-300nM for DAC treatment. Data indicated that 10nM of DAC had minimal effect on growth, gene expression, methylation or hydroxymethylation levels in either cell line. Figure 3A shows how the two cell lines responded differently to treatment. Vu40T cells were more susceptible to DAC with the density of cells after four days of 1μM DAC being considerably lower than the controls. Scc040 cells were also affected by treatment however this response was less evident (Figure 3A). The addition of RA to the treatments did not appear to have a significant effect (Figure 3B) and images allow for observations into differences between the two cell lines susceptibility to the drugs. MTT assays previously undertaken by the laboratory (unpublished/ personal communications) support these observations with IC50 established for both cell lines in response to DAC with Vu40T at 0.5-2.15μM and Scc040 above 9μM.

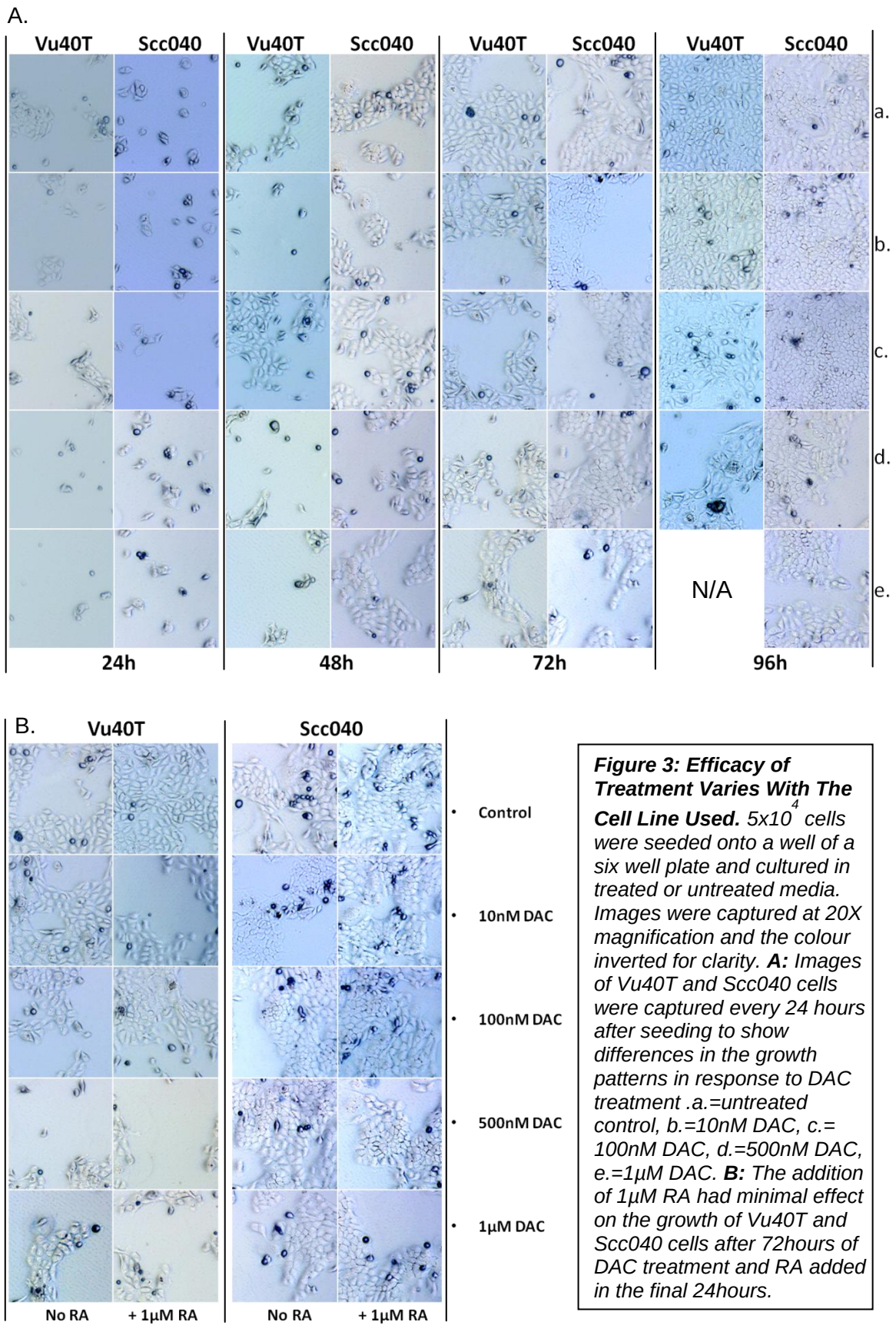

Figure 3: Efficacy of Treatment Varies With The Cell Line Used. *5x10^4 cells were seeded onto a well of a six well plate and cultured in treated or untreated media. Images were captured at 20X magnification and the colour inverted for clarity.* ***A:*** *Images of Vu40T and Scc040 cells were captured every 24 hours after seeding to show differences in the growth patterns in response to DAC treatment .a.=untreated control, b.=10nM DAC, c.= 100nM DAC, d.=500nM DAC, e.=1µM DAC.* ***B:*** *The addition of 1µM RA had minimal effect on the growth of Vu40T and Scc040 cells after 72hours of DAC treatment and RA added in the final 24hours.*

In Vu40T Cells DAC Treatment Causes a Reduction in Levels of 5mC and Increased Expression of RARβ

To determine the efficacy of DAC treatment slot blot analysis was applied determine the methylation status of DNA under different concentrations of DAC (Figure 4A). This entailed blotting 1000 or 500ng of DNA onto a nitrocellulose membrane and using an antibody to detect the presence 5mC. The results showed a gradual decrease in 5mC in keeping with the increase of DAC treatment confirming that DAC causes a reduction in global 5mC levels (Figure 4A). The addition of 9-cis retinoic acid appeared to slightly increase this reduction in 5mC though the mechanism(s) which account for this are unclear (Figure 4A). This may be an artefact of the slot blot technique which can be variable or it could be due to increased activation of the retinoic acid receptors and therefore increased expression of their various target genes, one of which may have an effect on the methylation status of the cells. The entire experiment was repeated twice and each sample was loaded into two separate wells of the slot blot manifold. ImageJ was used to quantify the intensity of each slot and combine all four results (Figure 4B). This is shown relative to the untreated control cells (Figure 4B).

This project aimed to determine the minimal dosage required to cause a decrease in methylation and reactivation of the tumour suppressor gene, RARβ. Quantitative PCR (qPCR) was used as quantifiable means of determining how gene expression changed in response to DAC treatment. For the Vu40T cells a dose-dependent increase in RARβ RNA was observed in response to DAC treatment suggesting that the RARβ promoter is methylated in untreated cells (Figure 4C). Two different genes were used as a control in this experiment: RARα

and GAPDH. GAPDH was used as it is known to be constitutively expressed and RARα was used for two reasons; one it is reported to be expressed constitutively and secondly RARβ activation is dependent upon its expression (Campos et al., 2009; de The et al., 1990). The 10nM concentration of DAC did not cause an increase in gene expression suggesting that the dose was too low to induce this. However 100nM DAC resulted in an almost a five-fold increase in RARβ RNA compared with the untreated cells when normalised to GAPDH and over double when normalised to RARα (Figure 4C). 1μM DAC resulted in 15X higher RARβ expression than untreated cells. The addition of 1μM RA increased RARβ expression with RA only cells having the same increase as was detected for 100nM DAC only treatment. Again 10nM exerted no effect but 100nM caused an increase in expression of almost 12 fold when combined with RA and 1μM DAC plus RA caused a 35 fold increase in gene expression (Figure 4C).

To examine the local effect of DAC on RARβ promoter methylation bisulfite conversion and restriction digest were performed. The bisulfite treatment converts unmethylated cytosines to uracil but leaves 5mC and 5hmC unaffected. After bisulfite conversion a 182 base pair fragment of the RARβ transcription start site was amplified using PCR and this product was digested with the Taqα1 restriction enzyme. The enzyme dissects the nucleotide sequence TCGA so if this site was methylated the sequence would remain TCGA after treatment and therefore be dissected at two locations generating three fragments of 76, 17 and 86 base pairs. However unmethylated DNA will be converted into TTGA and so will not be recognized by the enzyme leaving a single fragment of 182bp. This is summarised in figure 4E. The results of this experiment showed that the site is methylated in

untreated Vu40T cells as previously hypothesized and this methylation is removed with DAC treatment from as little as 100nM. The band intensity for 100nM appeared similar to that of 1μM suggesting that low dose DAC causes local changes in DNA methylation (Figure 4D).

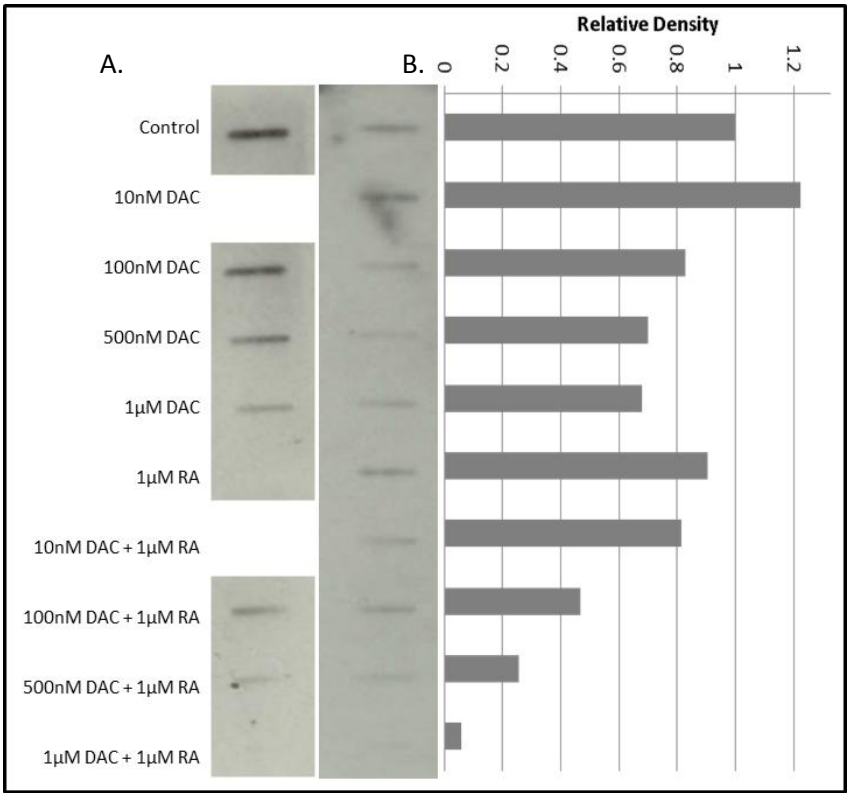
A.
B.
Relative Density
0
0.2
0.4
0.6
0.8
1
1.2
Control
10nM DAC
100nM DAC
500nM DAC
1µM DAC
1µM RA
10nM DAC + 1µM RA
100nM DAC + 1µM RA
500nM DAC + 1µM RA
1µM DAC + 1µM RA

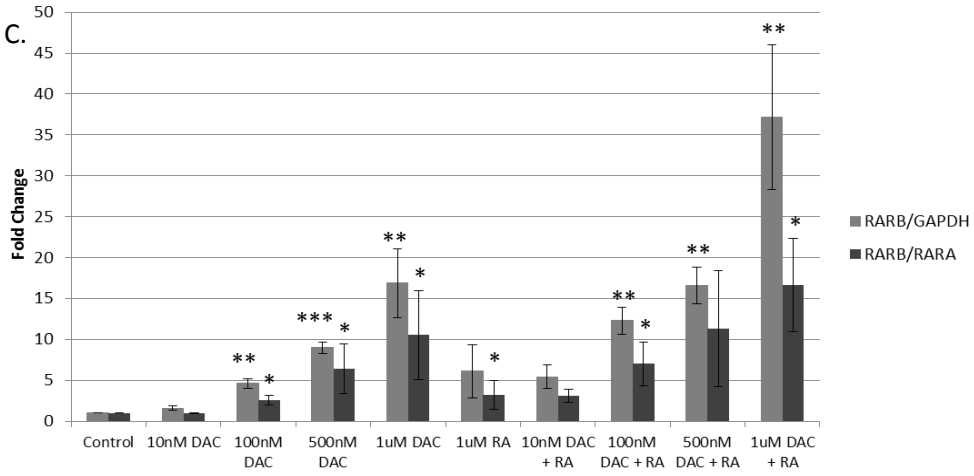
C.
Fold Change
50
45
40
35
30
25
20
15
10
5
0
Control
10nM DAC
100nM DAC
500nM DAC
1uM DAC
1uM RA
10nM DAC + RA
100nM DAC + RA
500nM DAC + RA
1uM DAC + RA
RARB/GAPDH
RARB/RARA

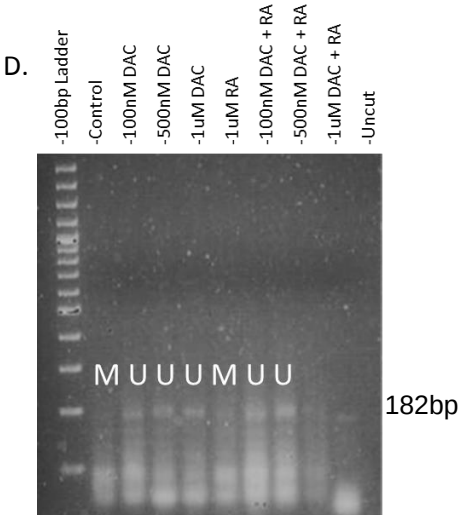
D.
-100bp Ladder
-Control
-100nM DAC
-500nM DAC
-1uM DAC
-1uM RA
-100nM DAC + RA
-500nM DAC + RA
-1uM DAC + RA
-Uncut
MUUUMUU
182bp

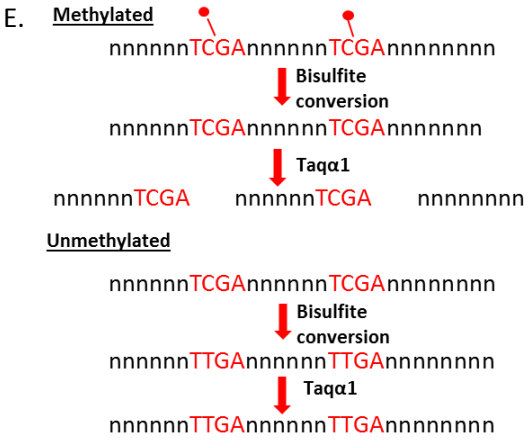
E.
Methylated
nnnnnnTCGAnnnnnnnTCGAnnnnnnnnn
Bisulfite conversion
nnnnnnTCGAnnnnnnnTCGAnnnnnnnn
Taqα1
nnnnnnTCGA
nnnnnnnTCGA
nnnnnnnn
Unmethylated
nnnnnnTCGAnnnnnnnTCGAnnnnnnnnn
Bisulfite conversion
nnnnnnTTGAnnnnnnnTTGAnnnnnnnnn
Taqα1
nnnnnnTTGAnnnnnnnTTGAnnnnnnnnn

Figure 4: 5'-Aza-2-deoxycytidine Treatment Causes a Decrease in Methylation and Subsequent Increase in RARβ Gene Expression in Vu40T Cells. *$5x10^4$ Vu40T cells were seeded onto one well of a six well plate either in normal cell culture medium or medium with the addition of 5'-Aza-2-deoxycytidine(DAC) at varying concentrations for 4 days with or without 1μM 9-cis retinoic acid(RA) for the final 2 days of culture. Each experiment was performed in duplicate.* ***A:*** *Slot blots show 5mC decreased with DAC treatment. DNA was blotted onto a nitrocellulose membrane using the slot blot manifold. This was exposed to a 5mC primary antibody. Duplicate analyses were performed for each DNA sample.* ***B:*** *ImageJ data analysis determining slot blot intensity from* ***A.*** *Results are the mean of two independent experiments and are shown here relative to the untreated control cells.* ***C:*** *RARβ gene expression increases in a dose-dependent manner. qPCR results show expression normalized to RARα and GAPDH presented as a fold change. Results are means obtained from two independent experiments. Error bars represent standard deviation and significance is determined by t-test against the untreated control cells. *=p<0.05, **=p<0.01, ***=p<0.005. Unmarked bars are not significant.* ***D-E:*** *The RARβ promoter is methylated in Vu40T cells. DNA was bisulfite converted then a region surrounding the transcription start site amplified by PCR. The PCR product was dissected using TaqαI at the sequence TCGA only in previously methylated samples. This product was then electrophorised on a 2% agarose gel. U=unmethylated, M=methylated. The band represents the 182bp uncut fragment.*

Scc040 Cells are Less Sensitive to DAC Treatment but May Respond to RA Alone.

The experiment was repeated in another HPV negative HNSCC cell line. Scc040 cells showed a higher resistance to DAC treatment as shown in Figure 3A and from previous results in the lab. However the slot blots analyses confirmed that the demethylating activity of 5-Aza-2'-deoxycytidine was effective in both cell lines (Figure 4A-B; 5A-B).

The results of the qPCR analyses showed that treatment with DAC alone had minimal effect on RARβ gene expression with 1μM DAC generating lower RARβ expression than the untreated cells (Figure 5C). However the addition of 1μM RA resulted in an increase in RARβ expression, with RA alone causing a three-fold increase which doubled when applied in combination with 1μM DAC (Figure 5C). When the initial levels of RARβ in the two cell types (Figure 5D) were compared Scc040 showed a higher basal expression than Vu40T. The bisulfite conversion

and restriction digest results show that treated Scc040 cells are at least partially unmethylated at the RARβ site however untreated cells and those treated only with 1μM DAC show faint bands at the 182bp size suggesting that some of the DNA may be unmethylated (Figure 5E).

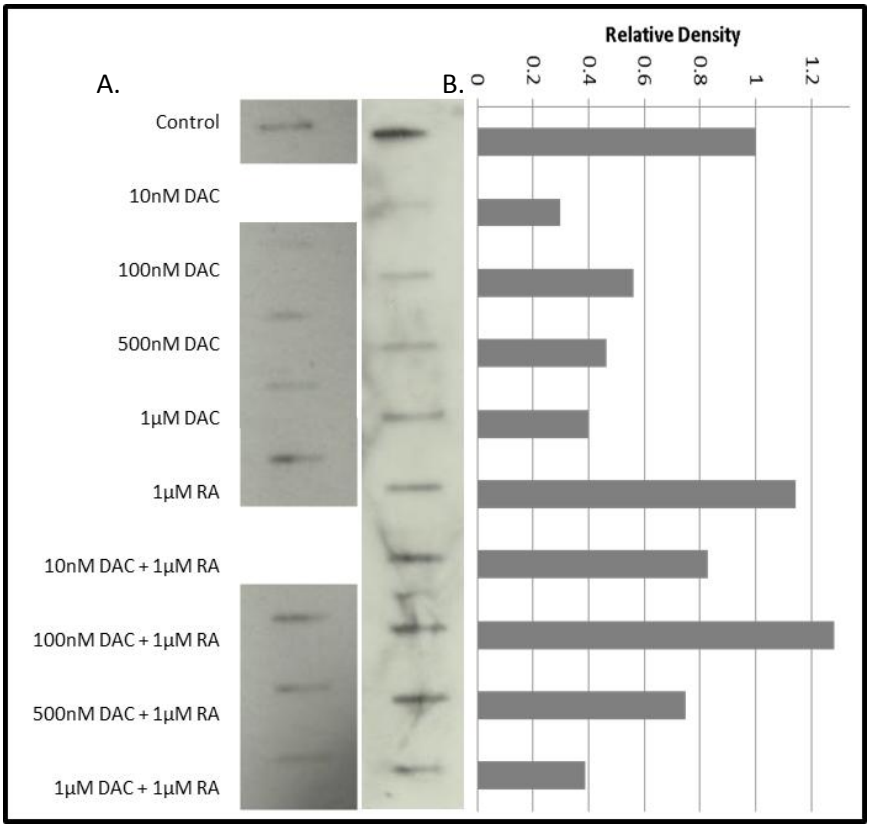
A.
B.
Relative Density
0
0.2
0.4
0.6
0.8
1
1.2
Control
10nM DAC
100nM DAC
500nM DAC
1µM DAC
1µM RA
10nM DAC + 1µM RA
100nM DAC + 1µM RA
500nM DAC + 1µM RA
1µM DAC + 1µM RA

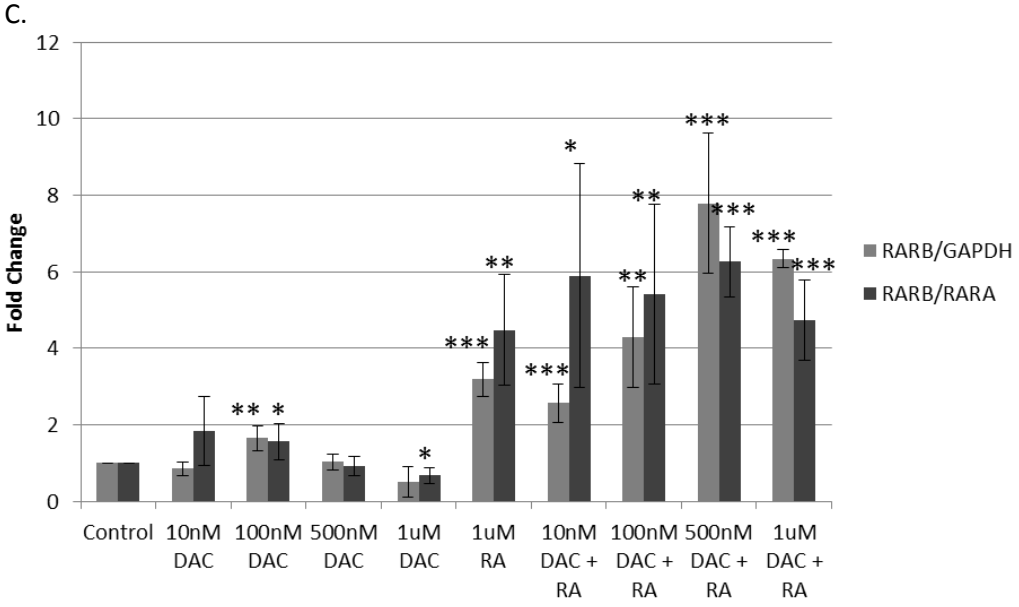
C.
Fold Change
RARB/GAPDH
RARB/RARA
Control
10nM DAC
100nM DAC
500nM DAC
1uM DAC
1uM RA
10nM DAC + RA
100nM DAC + RA
500nM DAC + RA
1uM DAC + RA

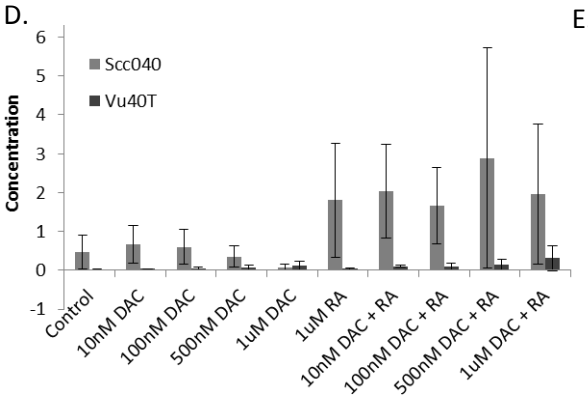
D.
Concentration
Scc040
Vu40T
Control
10nM DAC
100nM DAC
500nM DAC
1uM DAC
1uM RA
10nM DAC + RA
100nM DAC + RA
500nM DAC + RA
1uM DAC + RA

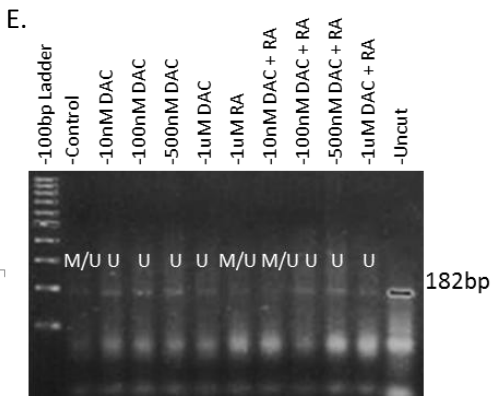
E.
-100bp Ladder
-Control
-10nM DAC
-100nM DAC
-500nM DAC
-1uM DAC
-1uM RA
-10nM DAC + RA
-100nM DAC + RA
-500nM DAC + RA
-1uM DAC + RA
-Uncut
182bp

Figure 5: 5'-Aza-2-deoxycytidine (DAC) Causes a Decrease in Global Methylation but RARβ Expression is Only Affected by 9-cis Retinoic Acid (RA) in Scc040 Cells. *5x104 Scc040 cells were plated onto 6 well plates and treated with varying concentrations of DAC for 4 days with or without 1μM RA for the final 2 days of culture.* ***A:*** *Slot blots of treated and untreated Scc040 DNA blotted onto a membrane and incubated with 5mC antibody overnight. Each sample was run twice.* ***B:*** *ImageJ data for slot blots from A shown as density of the bands for each treatment relative to the control sample. Results are the mean obtained from two independent experiments.* ***C****: qPCR results show that RARβ gene expression is increased by RA but not DAC treatment. Results are normalized to GAPDH and RARα and shown as a fold change. Results are the mean obtained from two experiments. Error bars show standard deviation. Significance is all in comparison with the untreated cells *=p<0.05, **=p<0.01, ***=p<0.005. Unmarked bars are not significant.* ***D:*** *Mean RARβ RNA concentrations for Scc040 and Vu40T cells under RA and DAC treatment. Results are normalized to RARα.* ***E:*** *Bisulfite converted DNA at the RARβ transcription start site was digested with Taqα1 restriction enzyme. Methylated samples (M) retain restriction site whereas unmethylated samples (U) remain uncut. The product was separated on a 2% agarose gel. The 182bp band represents the uncut fragment.*

DAC Increases Expression of TET2 Leading to an Increase in 5hmC Levels.

The effect of DAC and RA on levels of 5hmC was determined via slot blot analysis. 5hmC results from the oxidation of 5mC therefore 5mC must first be present in order to make 5hmC. Subsequently this lead to the initial hypothesis that treatment with DAC and therefore DNMT1 inhibition would lead to decreased levels of 5hmC as was seen for 5mC (Figures 4and 5A). However it was found that this was not the case, instead the global levels of 5hmC were increased in cells treated with higher concentrations of DAC (Figure 6A). This effect appeared in both cell lines and was only apparent in the highest concentrations examined with 10nM and 100nM having minimal or no effect. The levels of 5hmC in cancer cells has been reported previously to be very low (Jäwert et al, 2013) and this was confirmed in the slot blot results for both cell lines (Figure 6A). Additionally treatment with RA either alone or in combination with DAC resulted in an increase in 5hmC levels in both cell lines (Figure 6A).

In order to determine why this might be the case qPCR was performed on the same samples to identify corresponding changes in TET gene expression. The TET proteins are known to catalyse the conversion of 5mC to 5hmC so changes in TET gene expression in response to DAC treatment could account for the increase in 5hmC observed in the slot blots. Unfortunately the TET3 primers yielded no results so we were unable to determine the effect of DAC on TET3 expression. In Vu40T cells increasing the concentration of DAC above 10nM resulted in a decrease in TET1 gene expression (Figure 6B) either on its own or in combination with RA. Treatment with 100nM, 500nM and 1µM of DAC caused a reduction in TET1 RNA of over 60% (Figure 6B). TET1 expression in Scc040 cells was unaffected by DAC treatment (Figure 6C). TET2 however showed an increase in gene expression which correlated with the increase in 5hmC levels seen in the slot blots analysis (Figure 6D-E). In both cell lines increasing the concentration of DAC caused an increase in the levels of TET2 RNA. For Vu40T cells the observed increase in TET2 expression after treatment with 500nM and 1µM of DAC was 2.8 fold and 3.5 fold respectively (Figure 6D). TET2 expression in Scc040 cells was also dependent on DAC levels, both 100nM and 500nM DAC alone resulted in a doubling in TET2 mRNA, however 1µM DAC resulted in a fold change of almost 8 times (Figure 6E). The addition of RA increased these expressions however there was a large amount of variation between the replicates at the higher concentrations of DAC (Figure 6E). This result could be due to errors in the experimental procedure or may indicate that there is extreme variability in how sensitive Scc040 cells are to DAC and RA combined.

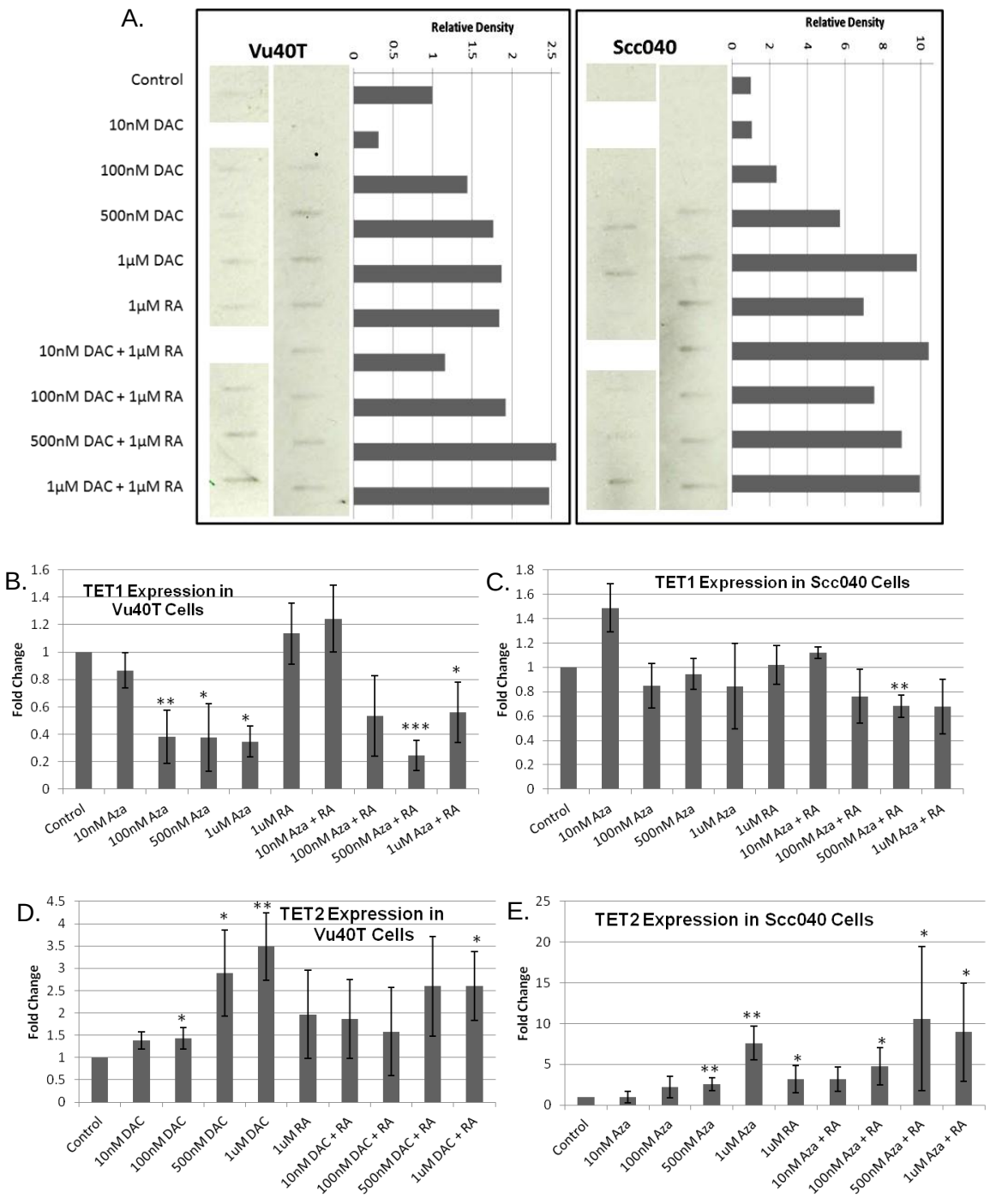

Figure 6: 5'-Aza-2-deoxycytidine (DAC) Increases Hydroxymethylcytosine Potentially Through Increased TET2 Gene Expression*. Vu40T and Scc040 cells grown in the presence of DAC for 4 days either alone or in combination with RA for 2 days. Every experiment was performed in duplicate.* ***A****: Slot blots showing 5hmC increases with DAC treatment. DNA was blotted onto a nitrocellulose membrane and incubated over night with the 5hmC antibody. Each DNA sample was run twice.* ***B-E****: qPCR results are normalized to GAPDH and shown as a fold change.* ***B:*** *TET1 expression in Vu40T cells.* ***C:*** *TET1 expression in Scc040 cells.* ***D:*** *TET2 expression in Vu40T cells.* ***E:*** *TET2 expression in Scc040 cells.*

Vu40T Cells Grown in Organotypic Raft Culture Express Very Low Levels of RARβ Which Decrease upon Treatment with DAC.

Growing cells in a monolayer is an efficient method however many aspects of these cells vary considerably from those *in vivo*. Therefore techniques which allow cells to grow and differentiate into 3D tissue have been developed and show gene expression profiles that resemble those of primary tissue more than their 2D counterparts (Ridky et al., 2010)**.** This project aimed to further determine whether cultivating Vu40T cells in a 3D tissue environment had any effect on the levels of RARβ expression or on the effectiveness of DAC treatment. The 3D culture system used entailed growing the cells on a collagen raft including encapsulated fibroblasts above a wire mesh on the surface of the media so that the cells were fed from below and in contact with air from above (Figure 7A). This is known as the air liquid interface.

The medium required for this system differed from the normal cell culture medium used in previous experiments. In order to make sure that Vu40T cells responded to DAC in the same way in this media (EMedia) the cells were either left untreated or treated with 100nM or 1μM of DAC in Emedia for four days and the expression of RARβ determined. Figure 7B shows the results of this experiment and it can be seen that DAC increases RARβ expression in EMedium in the same pattern as was previously observed (Figure 4C) but with even more dramatic fold changes detected.

Khan et al. (2012) recently showed that epithelial cells grown on raft cultures expressed similar levels of cytokeratins (CK) 5 and 6 to corresponding primary

tissue. These were used as markers of differentiation to clarify that the raft culture enabled the cells to differentiate. qPCR was performed using CK5 and CK6 primers on Vu40T cells grown in 2D and 3D culture. Both genes showed an increase in expression when grown in 3D culture in both treated and untreated cells with CK5 expression increased almost 25 times in the control cells indicating that the cells had differentiated (Figure 7C-D).

Four days prior to harvesting the raft cultures one culture was treated with 100nM DAC. This was added directly to the medium and so the cells were exposed to the drug from below. The 5mC slot blot results showed that the drug was taken up by the cells through this route as the level of 5mC decreased in the treated sample (Figure 7E). The 5hmC slot blot saw a corresponding increase, slightly higher than that observed in the 2D cultures (Figure 7E). The qPCR results showed that the 3D cultured cells expressed very little RARβ, none at all in the treated cells where GAPDH and RARα levels remained high (Figure 7F). RARβ expression in Vu40T cells appears always relatively low so this result could be due to inaccuracies in the qPCR and therefore further repeats are needed (Figure 7G).

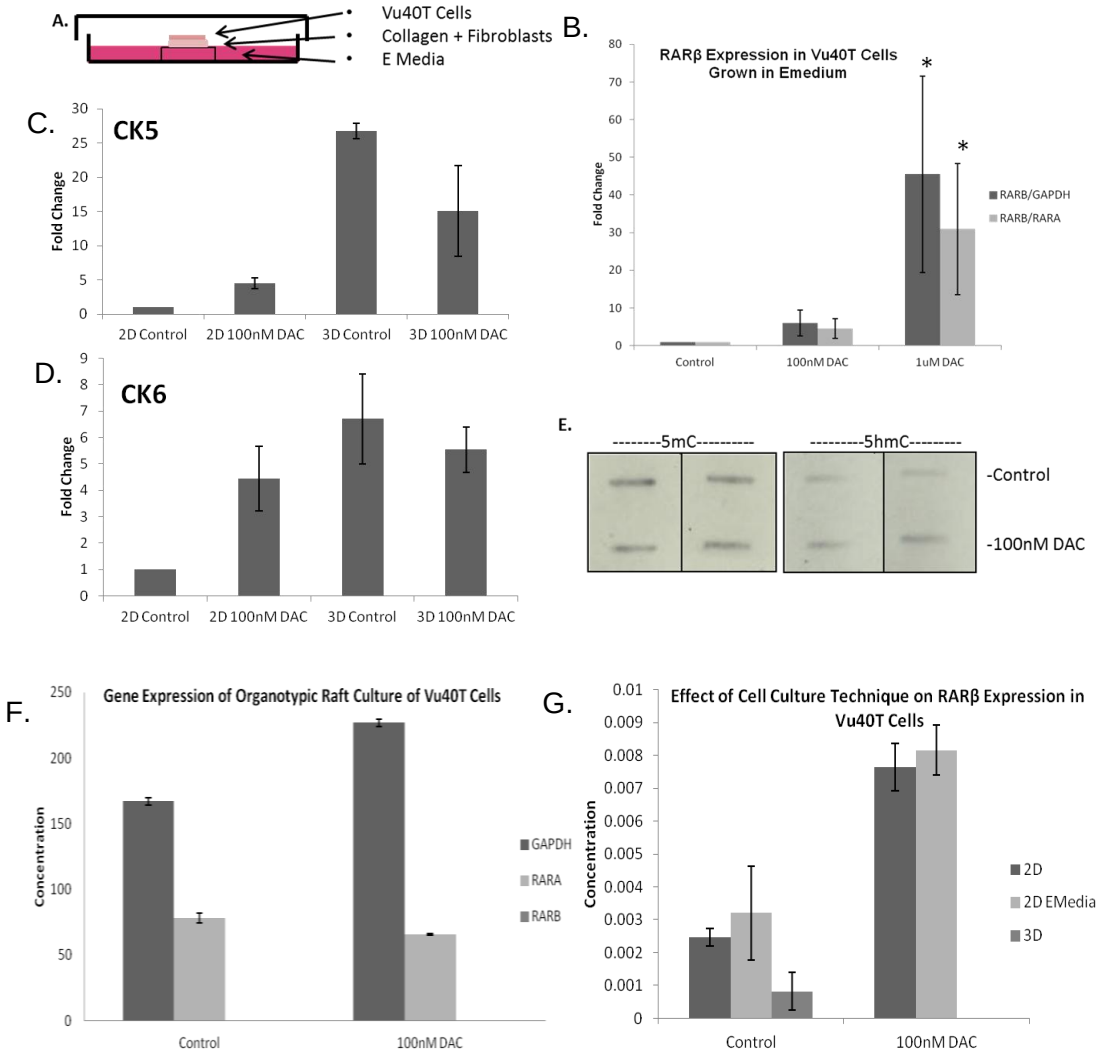

Figure 7: Organotypic Raft Culture of Vu40T Cells*. Vu40T cells were seeded onto a collagen raft embedded with fibroblasts. These were allowed to grow to confluence in the presence of Emedia. Once at confluence cultures were lifted onto a metal grid and grown at the air liquid interface for 11 days. 100nM of 5'-Aza-2-deoxycytidine (DAC) was added to the medium of one raft 4 days prior to harvest. Results shown are from a single experiment.* ***A:*** *diagrammatic representation of the raft culture system used.* ***B:*** *Vu40T cells were grown in Emedia (a specialised media for the 3D culture system) to determine whether the change in the media has any effect on the efficacy of DAC treatment. Results show the mean of two experiments, normalized to RARα or GAPDH and shown relative to the untreated cells.* ***C-D:*** *CK5 and 6 expression were used as biomarkers for differentiation. qPCR results show gene expression compared with GAPDH relative to the untreated monolayer cells. Both genes show an increase in expression when grown in the raft culture.* ***E:*** *Slot blot results for Vu40T cells grown in 3D. 1000ng DNA was blotted onto a nitrocellulose membrane and incubated with a 5mC or 5hmC antibody. 100nM DAC caused a minimal decrease in 5mC levels and a corresponding increase in 5hmC.* ***F:*** *Gene expression changes in Vu40T cells grown in organotypic raft culture in response to DAC treatment.* ***G:*** *RARβ expression in Vu40T cells grown in 3D raft culture, 2D monolayer in normal cell culture media or 2D monolayer in Emedia. RARβ expression was at minimally detectable levels in Vu40T cells when grown in the 3D culture system and decreased further following DAC treatment.*

Discussion

Cancer is a multifactorial disease with both genetic and epigenetic modifications contributing to its progression. For this reason therapeutic strategies involving the use of drugs which target aberrant epigenetic mechanisms such as HDAC inhibitors or demethylating agents are a promising pathway to pursue. Azacytidine (AZA) and its analogue 5-Aza-2'-deoxycytidine (DAC) have proven effective in the treatment of haematological malignancies and recent work suggests that the benefits of DAC treatment may be transferable to solid tumours (Issa et al., 2004, Leone et al., 2003, Kantarjian et al., 2006; Tsai et al., 2012). Both drugs act as demethylating agents that inhibit DNMT1 through their incorporation into DNA or RNA (Ghoshal et al., 2005). Progress in their use as anticancer drugs has been hindered by the fact that high doses can cause extreme toxicity however evidence suggests that low doses may have a therapeutic benefit without exerting the harmful side effects (Stressmann and Lyko, 2008). This project aimed to expand upon current knowledge of DAC treatment by treating oral cancer cell lines with varying concentrations of the drug either alone or in combination with retinoic acid.

The efficacy of any cancer therapeutic pathway is tumour specific and dependent on the genetic and epigenetic makeup of the cells. In order to get a broader view on the effectiveness of DAC treatment on oral cancer two separate HPV-negative OSCC cell lines were studied; Vu40T and Scc040. The effect of DAC treatment varied considerably between the two cell lines. For each cell line four different concentrations of DAC were used either in combination with RA or independently. Initial observations on cell growth (Figure 3A-B) demonstrated that Vu40Ts were

more affected by the drug than the Scc040 cells. This was confirmed by pervious MTT assays undertaken by the laboratory (Wiench- Personal communications) which found that the IC50 for Vu40Ts in response to DAC treatment to be considerably lower (0.5-2.15μM) than that of Scc040 cells (>9μM). In order to confirm the mechanism by which DAC exhorts its effect the global levels of methylation were determined via slot blot analysis. Results confirmed that DAC treatment reduced the global levels of DNA methylation in both cell lines (Figure 4A-B, 5A-B). Therefore although Scc040 cells appear more resistant to the cytotoxic effects of DAC the ability of the drug to demethylate DNA in this cell line was equal to that in Vu40T cells. A potential explanation for the difference in the efficacy of the drug is that Scc040 cells start with less aberrant methylation than Vu40T cells and the progression of the cancer was determined by other mechanisms such as genetic mutations or irregular chromatin states. Furthermore it would be interesting to determine whether there is any difference in DNMT1 gene expression between the two cell lines as this can confer resistance to DAC treatment.

RARβ is a tumour suppressor gene frequently silenced in solid tumours by epigenetic mechanisms (Connolly et al., 2013). In wild type cells its activation depends on retinoic acid binding to RARα which then induces the expression of RARβ as well as other target genes. Once active RARβ can mediate its own expression and activate its target genes. The main function of RARβ target genes is the control of cell differentiation and death (Connolly et al., 2013). Therefore when RARβ cannot be activated the cells evade death which is a hallmark of cancer (Hanahan and Weinberg, 2000). The expression of RARβ after treatment

with DAC was determined to provide a quantitative measure of the efficacy of the drug as we know that RARβ is methylated in many cancer cell types and hence its reactivation is an indication of the level of demethylation occurring. The addition of RA to the treatment model provides the cells with excess retinoic acid to activate the retinoic acid receptors. The qPCR results presented showed different patterns of RARβ gene activation for each cell line (Figure 4C-5C). Vu40T cells are highly susceptible to DAC treatment and the change in RARβ expression is in agreement with this observation. As the concentration of DAC increased so does the level of RARβ and this was heightened by the addition of RA (Figure 4C). Scc040 cells were less susceptible to treatment and demonstrate minimal change in RARβ expression when treated with DAC alone (Figure 5C). However the addition of RA caused a considerable increase in RARβ expression (Figure 5C). These results suggest that RARβ is methylated in Vu40T cells but not Scc040 cells and could partially explain why Scc040s are less susceptible to DAC treatment. This theory is supported when the levels of RARβ mRNA in Vu40T and Scc040 cells are compared (Figure 5D). The restriction digest results also showed higher levels of DNA methylation at the RARβ promoter in Vu40T cells than Scc040s however both cell lines demonstrated a decrease in methylation after DAC treatment (Figure 4D, 5E). Additionally both the Vu40T and Scc040 restriction digest gels allow for comparison of the 182bp uncut band but do not show clearly any of the digested fragments making determination of the methylation status less distinct. Therefore it would be beneficial to repeat the experiment, including investigation into other sites in the RARβ gene, using other restriction enzymes or using another site-specific method for determining methylation levels such as methylation sensitive PCR.

The addition of RA causes an increase in RARβ expression in both cell lines which is in agreement with the pathway to RARβ activation outlined above. RAR activation relies on ligand binding so pharmacological doses of RA mean more RA available to the cell (Connolly et al., 2013). Therefore RA has been considered as a potential therapeutic pathway to directly target the loss of RAR tumour suppression and in some cases is effective (Lotan et al, 1995). From these results I cannot state for certain that treating tumours which exhibit Scc040 cells characteristics with RA alone would provide an effective therapeutic strategy because the increase in RARβ expression seen may be in excess of what is required of a healthy cell. Repeating this experiment with a primary cell line from healthy oral epithelial cells may determine whether this is the case. However I can speculate that treating cancers with similar properties to Vu40T cells with DAC would have some therapeutic benefit via the reactivation of RARβ.

A further finding of this study was that 5hmC levels were increased with DAC treatment (Figure 6A). DAC demethylates DNA via incorporation into DNA in place of cytosine where it immobilizes and degrades DNMT1 (Stressmann and Lyko, 2008). This process was supported by the 5mC slot blot data which showed a dose dependent decrease in methylation in response to DAC treatment (Figure 4A-5A). 5mC is converted into 5hmC by the TET proteins; therefore the presence of 5hmC is 5mC dependent (Tahiliani et al., 2009). It could be hypothesised that when treated with DAC cells would show a reduction in 5hmC. However this was not the case and alternatively 5hmC increased with DAC treatment in both cell lines (Figure 6A). Although slot blots provide an overview of the methylation or

hydroxymethylation status of the DNA the technique is not very sensitive as the slots in the manifold can become blocked. As each sample was run twice and each experiment repeated this resulted in four slots per sample to obtain a mean from to provide a more accurate estimation of the levels of 5hmC or 5mC in each sample (Figures 4B, 5B, 6A). 5hmC has been reported to be low in oral cancer cells (Jäwert et al., 2013) and a similar result was observed here as both Vu40T and Scc040 untreated cells exhibited little to no 5hmC. This explains why the bands remain faint for all samples however it is clear that at 500nM and 1µM DAC more 5hmC is present for both cell types (Figure 6A). Unpublished immunofluorescence data (Wiench- personal communications) showed decreased 5hmC after DAC treatment for both cell lines confirming these findings.

In order to explain this unexpected observation qPCR was performed on cDNA from all the samples using primers specific for the TET1 and TET2 transcripts. As the TET hydroxylases are required for the conversion of 5mC into 5hmC increases in either gene might explain the data presented (Tahiliani et al., 2009). Results demonstrated that TET1 appeared to decrease by ~50% for Vu40T cells with a concentration of DAC above 100nM with or without RA, conversely Scc040 cells exhibited consistent levels of TET1 throughout the treatment (Figure 6B-C). Notably TET2 expression was at least doubled in both cell lines after treatment with DAC (Figure 6D-E). For Vu40T cells the effect of DAC on TET2 expression was only apparent after exposure to 500nM DAC when there was a 2.5 fold change from untreated cells, the same observation was seen when combined exposure with RA was applied (Figure 6D). Indeed treatment of Vu40T cells with RA alone also gave a slight increase in TET2 expression which corresponded with

the increased 5hmC levels seen in the slot blot analysis (Figures 6A-E). Interestingly Scc040 cells showed a more dramatic change in expression, after 100nM DAC exposure the TET2 RNA levels doubled and expression was 7 times that of the control at 1µM DAC (Figure 6E). The addition of RA increased all of these results with 500nM DAC + 1µM RA showing 10 times the amount of TET2 RNA as the control cells. These results identify a potential mechanism to explain how DAC treatment results in increased 5hmC levels. Although DAC leads to a decrease in the amount of 5mC via inhibition of DNMT1 it also causes an increase in TET2 expression which leads to more conversion of 5mC to 5hmC thereby increasing the levels of 5hmC (Figure 8). TET2 has already been shown to be decreased in oral cancers (Jäwert et al., 2013) so DAC treatment could provide a mechanism to bring about its reactivation and keep the levels of 5hmC high.

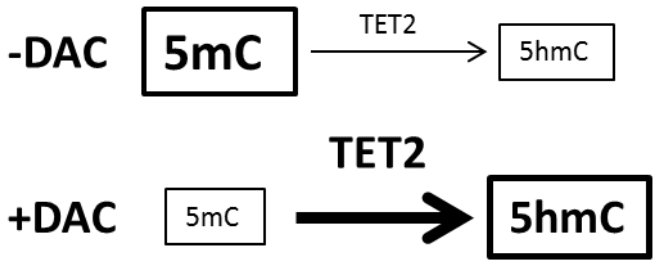

Figure 8: Schematic Representing a Potential Mechanism by which DAC Treatment Could Increase 5hmC Levels*. In the presence of DAC expression of TET2 is increased leading to an increase in the conversion of 5mC to 5hmC.*

5hmC is thought to be a step in the demethylation pathway however whether the modification has other functions remains unclear with some research suggesting that it may have functions beyond demethylation as distinct proteins bind to it and the other modified forms of cytosine (Iurlaro et al., 2013). Levels of 5hmC are reduced in various cancers; this may just be a biproduct of the increased 5mC commonly associated with cancer progression however it may suggest that the modification has tumour suppressive properties (Jäwert et al., 2013, Yang et al.,

2013). Likewise Yang et al. (2013) showed that the TET proteins are decreased in several tumours types and Jäwert et al. (2013) specifically showed a decrease in TET2 in oral cancer. Our results are in keeping with these findings and suggest that TET2 and 5hmC may function as tumour suppressors.

While the results presented here are preliminary, there are a number of further experiments which could be undertaken to confirm and expand upon our findings. Firstly the slot blot results would need to be confirmed with the use of another antibody. Additionally determining whether knock down of TET2 expression with si-RNA or an α-KG antagonist effects 5hmC levels after DAC treatment may help to confirm that TET2 reactivation causes the increase in 5hmC observed. Treating the cells with retinoic acid either alone or in combination with DAC caused an increase in the levels of 5hmC and TET2 in both cell lines (Figures 6A, 6D-E). Furthering these studies represents another area of future work. Firstly by determining whether any of the retinoic acid receptors are involved in regulation of TET2 gene expression, either by looking for the presence of RAREs in the TET2 promoter or performing chromatin immunoprecipitation with each RAR to see if the proteins are associated with the TET2 promoter. As the RARs have been associated with tumour suppression these results provide further support to the theory that 5hmC and TET2 are involved in tumour suppression (Connolly et al., 2013).

The results presented here have also shown that sensitivity to DAC is dependent on the cell line used. Furthermore the cell culture method used can contribute to the variation in the results as is seen from Figure 7. When grown using the 3D raft

culture technique Vu40T cells not only expressed considerably less RARβ but this expression decreased upon DAC treatment (Figure 7G) unlike the monolayer culture data which showed a consistent increase in RARβ expression after DAC exposure (Figure 4C). The 3D culture results are representative of a single experiment unlike the monolayer results and as such further organotypic culture experiments are warranted. However previous research has also shown differences in gene expression in monolayers versus 3D culture with the latter being closer to that of *in vivo* tumours (Ridky et al., 2010). This suggests that in order to determine the accuracy and relevance of monolayer results the experiment should be repeated using a 3D platform.

Conclusion

This project aimed to determine the effect of low dose 5-Aza-2'-deoxycytidine either in combination with 9-cis retinoic acid or alone on oral cancer cells lines. We showed that response to the treatment model was cell line dependent which mirrored the variability of cancer cells *in vivo*. Vu40T cells responded well to DAC treatment showing a gradual dose dependent increase in the expression of the tumour suppressor gene RARβ. Scc040 cells however were much less sensitive, showing an increase in RARβ expression only upon addition of RA to the treatment. This data may suggest that RARβ is epigenetically silenced in Vu40T cells but not in Scc040 cells. Furthermore DAC treatment lead to an increase in the global levels of 5hmC via increased TET2 gene expression. These results provide two mechanisms by which DAC exerts its effects in the treatment of oral cancer and suggest it may represent a promising therapeutic pathway to pursue.

Acknowledgments

With thanks to Dr Malgorzata Wiench, Harmeet Gill and Janine Fenton for all their help. And to Dr Sally Roberts for her help with the raft culture technique and Prof. Cooper and Dr. Scheven for their advice on writing the thesis.

References

Booth, M J., Ost T W B., Beraldi D., Bell N M., Branco M R., Reik W., and Balasubramanian, S. “Oxidative Bisulfite Sequencing of 5-Methylcytosine and 5-Hydroxymethylcytosine.” *Nature Protocols* 8, no. 10 (October 2013): 1841–1851. doi:10.1038/nprot.2013.115.

Campos, M S., Rodini C O., Pinto-Júnior D S., and Nunes F D. “GAPD and Tubulin Are Suitable Internal Controls for qPCR Analysis of Oral Squamous Cell Carcinoma Cell Lines.” *Oral Oncology* 45, no. 2 (February 2009): 121–126. doi:10.1016/j.oraloncology.2008.03.019.

Connolly, RM., Nguyen N K., and Sukumar S. “Molecular Pathways: Current Role and Future Directions of the Retinoic Acid Pathway in Cancer Prevention and Treatment.” *Clinical Cancer Research* 19, no. 7 (April 1, 2013): 1651–1659. doi:10.1158/1078-0432.CCR-12-3175.

de The, H., del Mar Vivanco-Ruiz, M., Tiollais,P., Stunnenberg,H., and Dejean, A. “Identification of a Retinoic Acid Responsive Element in the Retinoic Acid Receptor β gene.” *Nature* 343, no. 6254 (January 11, 1990): 177–180. doi:10.1038/343177a0.

Duong, V., and Rochette-Egly, C. “The Molecular Physiology of Nuclear Retinoic Acid Receptors. From Health to Disease.” *Biochimica et Biophysica Acta* 1812, no. 8 (August 2011): 1023–1031. doi:10.1016/j.bbadis.2010.10.007.

Gasche, J A., and Goel, A. “Epigenetic Mechanisms in Oral Carcinogenesis.” *Future Oncology (London, England)* 8, no. 11 (November 2012): 1407–1425. doi:10.2217/fon.12.138.

Ghoshal, K., Datta, J., Majumder, S., Bai, S., Kutay, H., Motiwala, T., and Jacob, S T. “5-Aza-Deoxycytidine Induces Selective Degradation of DNA Methyltransferase 1 by a Proteasomal Pathway That Requires the KEN Box, Bromo-Adjacent Homology Domain, and Nuclear Localization Signal.” *Molecular and Cellular Biology* 25, no. 11 (June 2005): 4727–4741. doi:10.1128/MCB.25.11.4727-4741.2005.

Hanahan, D, and Weinberg, R A. “The Hallmarks of Cancer.” *Cell* 100, no. 1 (January 7, 2000): 57–70.

He, Y-F., Li, B-Z., Li, Z., Liu, P., Wang, Y., Tang, Q., Ding, J., et al. “Tet-Mediated Formation of 5-Carboxylcytosine and Its Excision by TDG in Mammalian DNA.” *Science (New York, N.Y.)* 333, no. 6047 (September 2, 2011): 1303–1307. doi:10.1126/science.1210944.

Issa, J-P J., Garcia-Manero, G.,Giles, F J., Mannari, R., Thomas, D., Faderl, S., Bayar, E. et al. “Phase 1 Study of Low-Dose Prolonged Exposure Schedules of the Hypomethylating Agent 5-Aza-2′-Deoxycytidine (decitabine) in Hematopoietic Malignancies.” *Blood* 103, no. 5 (March 1, 2004): 1635–1640. doi:10.1182/blood-2003-03-0687.

Ito, S., Shen, L., Dai, Q., Wu, S C., Collins,L B., Swenberg, J A., He, C., and Zhang, Y. “Tet Proteins Can Convert 5-Methylcytosine to 5-Formylcytosine and 5-Carboxylcytosine.” *Science (New York, N.Y.)* 333, no. 6047 (September 2, 2011): 1300–1303. doi:10.1126/science.1210597.

Iurlaro, M., Ficz, G., Oxley, D., Raiber, E-A., Bachman, M., Booth,M J., Andrews, S., Balasubramanian, S and Reik, W. “A Screen for Hydroxymethylcytosine and Formylcytosine Binding Proteins Suggests Functions in Transcription and Chromatin Regulation.” *Genome Biology* 14, no. 10 (2013): R119. doi:10.1186/gb-2013-14-10-r119.

Jäwert, F, Hasséus, B., Kjeller, G., Magnusson, B., Sand, L., and Larsson, L. “Loss of 5-Hydroxymethylcytosine and TET2 in Oral Squamous Cell Carcinoma.” *Anticancer Research* 33, no. 10 (October 2013): 4325–4328.

Jüttermann, R, Li, E., and Jaenisch, R. “Toxicity of 5-Aza-2’-Deoxycytidine to Mammalian Cells Is Mediated Primarily by Covalent Trapping of DNA Methyltransferase rather than DNA Demethylation.” *Proceedings of the National Academy of Sciences of the United States of America* 91, no. 25 (December 6, 1994): 11797–11801.

Jithesh, P V., Risk, J M., Schache, A G., Dhanda, J., Lane, B., Liloglou, T and Shaw, R J. “The Epigenetic Landscape of Oral Squamous Cell Carcinoma.” *British Journal of Cancer* 108, no. 2 (February 5, 2013): 370–79. doi:10.1038/bjc.2012.568.

Kantarjian, H., Issa J-P J., Rosenfeld, C S., Bennett, J M., Albitar, M., DiPersio, J., Klimek, V., et al. “Decitabine Improves Patient Outcomes in Myelodysplastic Syndromes: Results of a Phase III Randomized Study.” *Cancer* 106, no. 8 (April 15, 2006): 1794–1803. doi:10.1002/cncr.21792.

Khan, E., Shelton, R M., Cooper, P R., Hamburger, J., and Landini, G. “Architectural Characterization of Organotypic Cultures of H400 and Primary Rat Keratinocytes.” *Journal of Biomedical Materials Research Part A* 100A, no. 12 (2012): 3227–3238. doi:10.1002/jbm.a.34263.

Klose, R J., and Bird, A P. “Genomic DNA Methylation: The Mark and Its Mediators.” *Trends in Biochemical Sciences* 31, no. 2 (February 2006): 89–97. doi:10.1016/j.tibs.2005.12.008.

Leone, G., Voso, M T., Teofili, L and Lübbert, M. “Inhibitors of DNA Methylation in the Treatment of Hematological Malignancies and MDS.” *Clinical Immunology* 109, no. 1 (October 2003): 89–102. doi:10.1016/S1521-6616(03)00207-9.

Lotan, R, Xu, X-C., Lippman, S M., Ro, J Y., Lee, J S., Lee, J J., and Hong, W K. “Suppression of Retinoic Acid Receptor–β in Premalignant Oral Lesions and Its Up-Regulation by Isotretinoin.” *New England Journal of Medicine* 332, no. 21 (1995): 1405–1411. doi:10.1056/NEJM199505253322103.

Mayer, W., Niveleau, A., Walter, J., Fundele, R., and Haaf, T. “Embryogenesis: Demethylation of the Zygotic Paternal Genome.” *Nature* 403, no. 6769 (February 3, 2000): 501–502. doi:10.1038/35000656.

McCaffrey, L M., and Macara, I G. “Epithelial Organization, Cell Polarity and Tumorigenesis.” *Trends in Cell Biology* 21, no. 12 (December 2011): 727–735. doi:10.1016/j.tcb.2011.06.005.

Neville, B W., and Day, T A. “Oral Cancer and Precancerous Lesions.” *CA: A Cancer Journal for Clinicians* 52, no. 4 (2002): 195–215. doi:10.3322/canjclin.52.4.195.

Piccolo, F M., and Fisher, A G. “Getting Rid of DNA Methylation.” *Trends in Cell Biology*. Accessed January 26, 2014. doi:10.1016/j.tcb.2013.09.001.

Raffoux, E., Cras, A., Recher, C., Boëlle, P-Y., de Labarthe, A., Turlure, P., Marolleau, J-P., et al. “Phase 2 Clinical Trial of 5-Azacitidine, Valproic Acid, and All-Trans Retinoic Acid in Patients with High-Risk Acute Myeloid Leukemia or Myelodysplastic Syndrome.” *Oncotarget* 1, no. 1 (May 2010): 34–42.

Ridky, T W., Chow, J M., Wong, D J., and Khavari, P A. “Invasive 3-Dimensional Organotypic Neoplasia from Multiple Normal Human Epithelia.” *Nature Medicine* 16, no. 12 (December 2010): 1450–1455. doi:10.1038/nm.2265.

Schneider, C A., Rasband, W S., and Eliceiri, K W. “NIH Image to ImageJ: 25 Years of Image Analysis.” *Nature Methods* 9, no. 7 (July 2012): 671–75. doi:10.1038/nmeth.2089.

Sciubba, J J. “Oral Cancer. The Importance of Early Diagnosis and Treatment.” *American Journal of Clinical Dermatology* 2, no. 4 (2001): 239–251.

Stresemann, C., and Lyko, F. “Modes of Action of the DNA Methyltransferase Inhibitors Azacytidine and Decitabine.” *International Journal of Cancer. Journal International Du Cancer* 123, no. 1 (July 1, 2008): 8–13. doi:10.1002/ijc.23607.

Tahiliani, M., Koh, K P., Shen, Y., Pastor, W A., Bandukwala, H., Brudno, Y., Agarwal, S., et al. “Conversion of 5-Methylcytosine to 5-Hydroxymethylcytosine in Mammalian DNA by MLL Partner TET1.” *Science (New York, N.Y.)* 324, no. 5929 (May 15, 2009): 930–935. doi:10.1126/science.1170116.

Tan, Li, and Yujiang Geno Shi. “Tet Family Proteins and 5-Hydroxymethylcytosine in Development and Disease.” *Development (Cambridge, England)* 139, no. 11 (June 2012): 1895–1902. doi:10.1242/dev.070771.

Tsai, H-C, Li, H., Van Neste, L., Cai, Y., Robert, C., Rassool, F V., Shin, J J., et al. “Transient Low Doses of DNA-Demethylating Agents Exert Durable Antitumor Effects on Hematological and Epithelial Tumor Cells.” *Cancer Cell* 21, no. 3 (March 20, 2012): 430–446. doi:10.1016/j.ccr.2011.12.029.

Tsai, H-C, and Baylin, S B. “Cancer Epigenetics: Linking Basic Biology to Clinical Medicine.” *Cell Research* 21, no. 3 (March 2011): 502–517. doi:10.1038/cr.2011.24.

Wilson, R, Fehrmann, F., and Laimins, L A. “Role of the E1-E4 Protein in the Differentiation-Dependent Life Cycle of Human Papillomavirus Type 31.” *Journal of Virology* 79, no. 11 (June 2005): 6732–6740. doi:10.1128/JVI.79.11.6732-6740.2005.

Yang, H, Liu,Y., Bai, F., Zhang, J-Y., Ma, S-H., Liu, J., Xu, Z-D., et al. “Tumor Development Is Associated with Decrease of TET Gene Expression and 5-Methylcytosine Hydroxylation.” *Oncogene* 32, no. 5 (January 31, 2013): 663–669. doi:10.1038/onc.2012.67.

UNIVERSITY OF BIRMINGHAM
COLLEGE OF MEDICINE AND DENTISTRY

PROJECT 2

The Respiratory Phenotype of *Phd1*$^{-/-}$ Mouse Liver Mitochondria

---

Hannah Jessica Eadie

Supervisor: Dr D. Tennant

May 2014

This project is submitted in partial fulfilment of the requirements for the award of the MRes.

Abstract

Hypoxia inducible factor (HIF) is the master regulator of the hypoxia response. The active form is composed of two subunits (α and β), in the presence of oxygen the alpha subunit is constantly degraded. HIF-α stability is controlled by the HIF prolyl hydroxylase domain proteins (PHDs) in an oxygen dependent process. Phd1 knockout mice show a shift in metabolism to produce more ATP through glycolysis and consume less oxygen. The aim of this project was to determine the respiratory phenotype of $Phd1^{-/-}$ mouse liver mitochondria. The results showed that loss of PHD1 altered the activity of mitochondrial complexes I-IV in a highly variable manner. Therefore the pathway from Phd1 knockout to decline in mitochondrial complex function is not a linear one. PHD1 can be induced by oestrogen and this project suggests that the effect of PHD1 loss on mitochondrial decline may be sex specific.

Introduction

The Role of Mitochondria in ATP Production

Mitochondria produce 90% of cellular ATP. This is dependent upon an electrochemical gradient across the inner mitochondrial membrane created by respiratory complexes I-IV. The redox potential of the initial electron donor NADH is -340mV whereas O_2, the final acceptor, has a redox potential of +810mV (Mailloux et al., 2013).Therefore the transfer of electrons from NADH to O_2 is an energetically favourable process. This drives the transfer of protons across the inner membrane and creates the proton motif force (PMF) providing the energy required to fuel ATP production (Mailloux et al., 2013).

Complex 1 (NADH dehydrogenase) spans the inner membrane. It shuttles two electrons from NADH to ubiquinone (Q) generating NAD and ubiquinol (QH2) (Davis and Williams, 2012). Succinate dehydrogenase or complex II transfers electrons from succinate to the Q pool via flavin adenine dinucleotide (FAD) (Davis and Williams, 2012). Electrons from QH2 are then transferred to cytochrome C by complex III (ubiquinol-cytochrome c (CytC) reductase). Finally Complex IV (cytochrome C oxidase) transfers electrons from cytochrome C to the final electron acceptor oxygen to create water (Mailloux et al., 2013; Davis and Williams, 2012). Complexes I, III and IV span the inner mitochondrial membrane and the transfer of electrons from NADH to O_2 releases the energy required for them to pump protons (H^+) across the membrane into the intermembane space (Wei et al., 2009). This proton gradient is harnessed by complex V, the F1F0 ATP

synthase to convert ADP to ATP (Mailloux et al., 2013). This is summarised in Figure1.

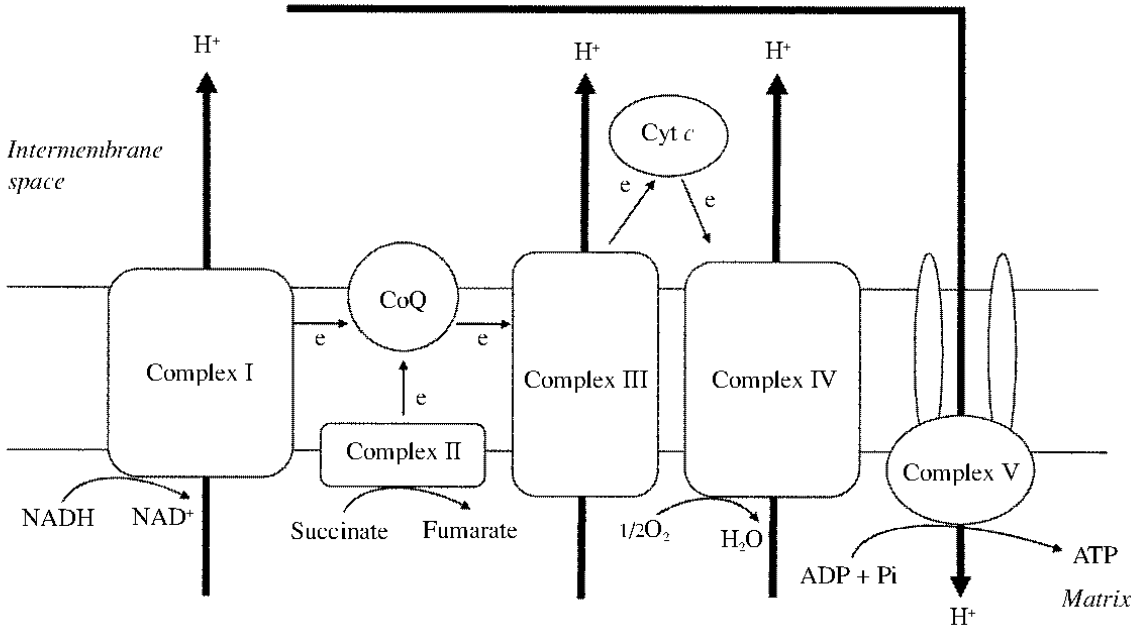

Subunits	Complex I	Complex II	Complex III	Complex IV	Complex V
mtDNA-encoded	7	0	1	3	2
nDNA-encoded	36	4	10	10	14

Figure 1: The Electron Transport Chain (ETC): *Figure from Wei et al. (2009). The ETC spans the inner mitochondrial membrane and uses a series of redox reaction to fuel the transfer of protons accross the membrane. Complex I or NADH dehydrogenase converts NADH to NAD^+ and passes the electron to ubiquinone. Complex II (Succinate dehydrogenase) transfers electrons from succinate to the Q pool to generate fumerate. Complex III(ubiquinol-cytochrome c reductase) then transfers electrons from Q to cytochrome c (Cyt c). These are then taken by complex IV(cytochrome c oxidase) to generate H_2O from O_2. This process is energetically favourable so complexes I, III and IV use the energy released to pump protons across the membrane creating the proton motif force (PMF). The PMF is a store of energy which can be harness by complex V (ATP synthase) to generate ATP from ADP + Pi. Subunits of the mitochondrial complexes are encoded by a mix of nuclear (n) DNA and mitochondrial (mt) DNA.*

ROS Production in the Mitochondria

Mitochondria are also major producers of reactive oxygen species (ROS) (Shigenaga et al., 1994). The organelles are present in relatively high numbers, consume the most cellular oxygen and are rich in redox carriers (Shigenaga et al., 1994; Andreyev et al., 2005). Therefore the organelles link to ROS production is inevitable. Complex I and complex III are the best characterized producers of

ROS in the mitochondria although various other proteins also contribute (Andreyev et al., 2005). In the ETC electrons from complexes I and III (and occasionally II) can be released prematurely generating superoxide (O_2^-) (Andreyev et al., 2005). This is converted into hydrogen peroxide (H_2O_2), the main species of ROS (Mailloux et al., 2013). H_2O_2 has a long half-life, can diffuse through membranes and is involved in various processes such as insulin signalling and response to hypoxia (Mailloux et al., 2013). However accumulation of H_2O_2 and O_2^- can lead to the damage of DNA, RNA and proteins in various ways: they can lead to the production of the hydroxyl radical (OH) that indiscriminately oxidizes macromolecules; H_2O_2 can inactivate proteins by oxidizing redox-sensitive thiol groups; when combined with nitric oxide, O_2^- forms the very toxic peroxynitrite species; or alone O_2^- can disassemble iron-sulphur clusters causing damage to TCA cycle enzymes and respiratory complexes (Mailloux et al., 2013). As the main site of ROS production, mitochondria are particularly prone to damage by ROS. A number of respiratory enzymes are encoded by DNA in the mitochondria (mtDNA) (Figure 1). Mutations are more frequent in mtDNA than nuclear DNA due to lack of protection by histones; less effective DNA repair systems and proximity to the site of ROS production (Wei et al., 2008). Therefore mitochondrial damage by ROS is two-fold; the proteins can be damaged directly or ROS can cause mutations in mtDNA leading to irreversible damage which is heritable across cellular generations (Wei et al., 2008).

High mitochondrial membrane potential is linked to increased production of ROS and so one mechanism to limit accumulation of ROS is through uncoupling proteins (UCP1-3) (Korshunov et al., 1997; Mailloux and Harper, 2011). UCPs

transport ions across the inner mitochondrial membrane reducing the electrochemical gradient produced by the electron transport chain (Donadelli et al., 2013). UCPs are thought to leak protons across the membrane in order to prevent ROS emission, a theory confirmed by the excess ROS production seen in *Ucp2* $^{-/-}$ mice (Mailloux and Harper, 2011).

Mitochondria and Aging

Since the 1950's theories have linked ROS accumulation and subsequent mitochondrial damage with the natural process of aging (Harman, 1956; Wei et al., 2008). In young, healthy cells ROS are a natural biproduct of respiration but antioxidants and free radical scavenger enzymes prevent their accumulation (Wei et al., 2008). However as cells age the production of superoxide anions and H_2O_2 increases and the capacity of antioxidants and free radical scavengers to remove them decreases (Wei et al., 2008). This leads to the accumulation of free radicals, subsequent damage to mitochondria, a shift in respiration efficiency and an increase in ROS production creating a vicious cycle of mitochondrial decline (Wei et al., 2008). Aged cells demonstrate an accumulation of mtDNA mutations, mitochondrial structural damage and a reduction in respiratory enzyme activity (Bandy and Davidson, 1990; Wei et al., 2008). Senescent fibroblasts from human skin and lung demonstrate decreased pyruvate dehydrogenase activity (PDC) and increased pyruvate dehydrogenase kinase (PDK) after treatment with H_2O_2 (Wei et al., 2008). PDC is required for the conversion of pyruvate to acetyl CoA and hence this reduction in activity will decrease entry of glycolytic intermediates into the TCA cycle and increase glycolytic production of ATP (Wei et al., 2008).

The Role of PHDs in the Control of HIF-α Stability

In order to protect against hypoxia cells must induce the expression of numerous genes to reprogram metabolism and increase angiogenesis and erythropoiesis (Fong et al., 2008). This change in gene expression is controlled in the most part by hypoxia-inducible factor (HIF). The transcription factor is composed of two subunits α and β, under hypoxia these heterodimerize and bind to hypoxia response elements (HREs) where they induce the expression of their target genes (Applehoff et al., 2004). In normoxia the alpha subunit (HIF-1α, HIF-2α, HIF-3α) is constitutively expressed but constantly degraded by the proteasome (Applehoff et al., 2004; Bruik and McKnight, 2001). This degradation is controlled by a family of HIF prolyl hydroxylase domain proteins (PHD1, PHD2 and PHD3, also called ElgNs or HPHs) (Bruik and McKnight, 2001). The PHDs are Fe^{2+} and 2-oxoglutarate-dependent dioxygenases and are highly sensitive to changes in cellular oxygen concentration (Kaelin and Ratcliffe, 2008). They hydroxylate prolines 564 and 402 on HIF-α creating a binding site for the von Hippel Lindau protein (VHL) which polyubiquitinates HIF-α targeting it for proteasomal degradation (Figure 2) (Papandreou et al., 2006).

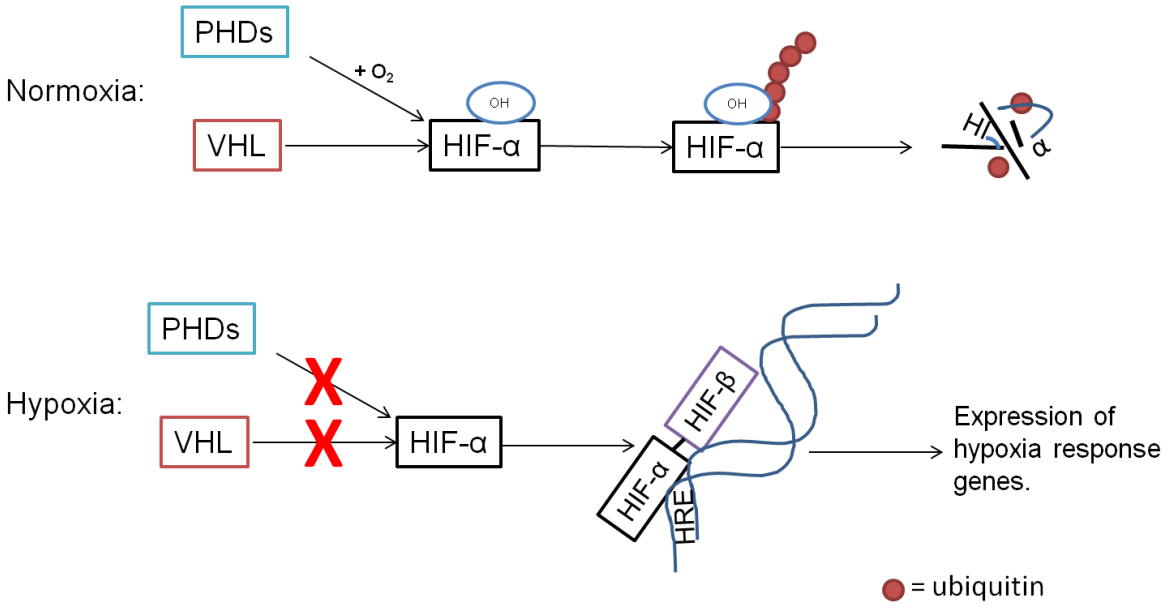

Figure 2: The role of the PHD proteins in HIF-α control. *In the presence of oxygen PHD proteins (1,2 or 3) use oxygen to hydroxylate HIF-α (1,2, or 3). This hydroxylation allows the von Hippel Lindau (VHL) protein to bind and polyubiquitinate HIF-α targeting it for degradation by the proteasome. In hypoxia PHDs cannot hydroxylate HIF-α so VHL cannot bind. HIF-α is therefore not degraded and can heterodimerize with HIF-β and induce the expression of genes downstream of hypoxia response elements (HREs). These bring about a change in metabolism, increased angiogenesis and erythropoiesis and reduced consumption of oxygen.*

PHD1

The three PHDs all have the ability to hydroxylate HIF-α and induce HRE gene expression *in vivo* however they differ slightly in terms of function, activation and cellular location (Appelhoff et al., 2004; Metzan et al., 2003). Takeda et al. (2006) looked at the effect of knocking out each of the PHDs in mouse embryonic development and found that Phd1 and 3 knockouts were viable but *Phd2*$^{-/-}$ mice were embryonic lethal. PHD2 is the most abundant and thought to be the main regulator of HIF-1α (Appelhoff et al., 2004). However the focus of this report is on PHD1. Unlike the other PHDs PHD1 is found exclusively in the nucleus and exhorts its effects mainly on HIF-2α in normoxia (Metzen et al., 2003; Appelhoff et al., 2004).

The gene was found independently by Seth et al. (2002) (referred to as EIT-6) in a screen for oestrogen dependent genes in a breast cancer cell line and shown to be a direct transcriptional target of the oestrogen receptor. In breast cancer cell lines, overexpression of Phd1 causes resistance to tamoxifen and leads to oestrogen independent growth linking PHD1 to oestrogen regulation and breast cancer progression (Seth et al., 2002). Appelhoff et al. (2004) confirmed this link as they found a 2.5 fold increase in protein levels after stimulation with oestrogen. Zhang et al., (2009) used siRNA to knock down PHD1 activity in various cell lines and found that this decreased cyclin D1 mRNA and protein levels and suppressed mammary gland proliferation. Inhibition of PHD2 or 3 had no effect (Zhang et al., 2009). Furthermore this function of PHD1 appears to be HIF-independent as knock down of PHD1 had no effect on levels of either HIF-α protein and knocking down or overexpressing HIF-2α had no effect on the levels of cyclin DI in PHD1 deficient cells (Zhang et al., 2009). The hydroxylase function of PHD1 however is still required to control the levels of cyclin D1 and therefore this process is oxygen dependent (Zhang et al., 2009). Similarly PHD1 has been seen to be involved in regulation of transcription factor NF-kB and centrosomal protein Cep192 in HIF-independent processes (Cummins et al., 2006; Moser et al., 2013). These results show that PHD1 has functions beyond the control of HIF-2α.

Phd1 knockout mice show reduced oxygen consumption and a shift in basal metabolism similar to that seen under conditions of hypoxia and in aged cells (Aragonés et al., 2008; Wei et al., 2008). Pyruvate dehydrogenase kinases (PDKs) inhibit PDC which is required for progression into the TCA cycle

(Aragonés et al., 2008). Aragonés et al. (2008) found that loss of PHD1 in skeletal muscle resulted in an increase in pdk1 and 4 at the mRNA and protein levels; this corresponded with a 54% reduction of PDC activity. The overall result of this is an increase in glycolytic production of ATP as glycolytic intermediates are prevented from entry into the TCA cycle (Aragonés et al., 2008). Schneider et al. (2010) made a similar discovery in the livers of *Phd1*$^{-/-}$ mice. Both papers linked this shift in metabolism to protection against acute ischemia, a phenotype specific to *Phd1*$^{-/-}$ as knock out of the other PHD genes did not have the same effect (Aragonés et al., 2008; Schneider et al., 2010). An increase in the levels of transcription factor Pparα was also observed (Aragonés et al., 2008). As this is known to regulate pdk4 it provides a potential step in the pathway from Phd1 knockout to increased glycolysis. These papers propose that HIF-2α mediates this response as *Phd1*$^{-/-}$ mice show increased HIF-2α protein levels and when crossed with *Hif-2α* $^{+/-}$ mice the ischemia protection is lost (Aragonés et al., 2008).

Aims and Objectives

This project aims to determine the respiratory phenotype of mitochondria from Phd1 knockout mouse livers. The main objectives are to:

-Isolate mitochondria from wild type and *Phd1*$^{-/-}$ mouse livers;

-Determine the activity of respiratory complexes I-IV in these mitochondria;

-Compare the effect of the age and sex of the mice used on these results.

Materials and Methods

DNA Extraction from Mouse Ear Clips

To each ear clip 200µl TNES buffer (5ml=500µl 100mM Tris, 800µl 2.5M sodium chloride (NaCl), 1ml 0.5M ethylenediaminetetraacetic acid (EDTA), 300µl 10% sodium dodecyl sulphate (SDS), dH_2O) + 15µl Proteinase K (1mg/100µl) was added. These were incubated at 65^oC for 3 hours. 56µl of 5M NaCl was added to each sample, vortexed and then centrifuged at 4^oC at 14000g for 20 minutes. The supernatant was transferred to a new tube and two volumes of 100% ethanol added to precipitate the DNA. This was then centrifuge at 14000g for 10 minutes, the supernatant discarded and pellet washed in 70% ethanol. Once dried the DNA pellet was resuspended overnight at 37^oC in 10mM Tris.

Genotyping

The mouse model used is described elsewhere and summarised in figure 3 (Aragonés et al., 2008). To genotype the samples two PCRs were performed. One was using primers against exon 4 of the Phd1 gene (present in heterozygous and wild type animals) and one using primers against the inserted neomycin cassette (present in heterozygote and knockout animals). The PCR mix remained constant (2µl 20mM primers, 10µl MyTaq Buffer, 0.625µl MyTaq polymerase, 50ng DNA, dH_2O) .The programme varied depending on the primer pair. For neomycin: 95^oC for 1 minute, then 30 cycles of 95^oC for 15 seconds, 65^oC for 15 seconds and then 72^oC for 10 seconds, followed by 1 minute at 72^oC. For exon 4 the PCR programme was the same with the exception that the annealing temperature was changed to 60^oC.

Products were run on a 1.5% (neomycin) or 2% (exon 4) agarose gel in 1X TAE for 20 minutes at 100V.

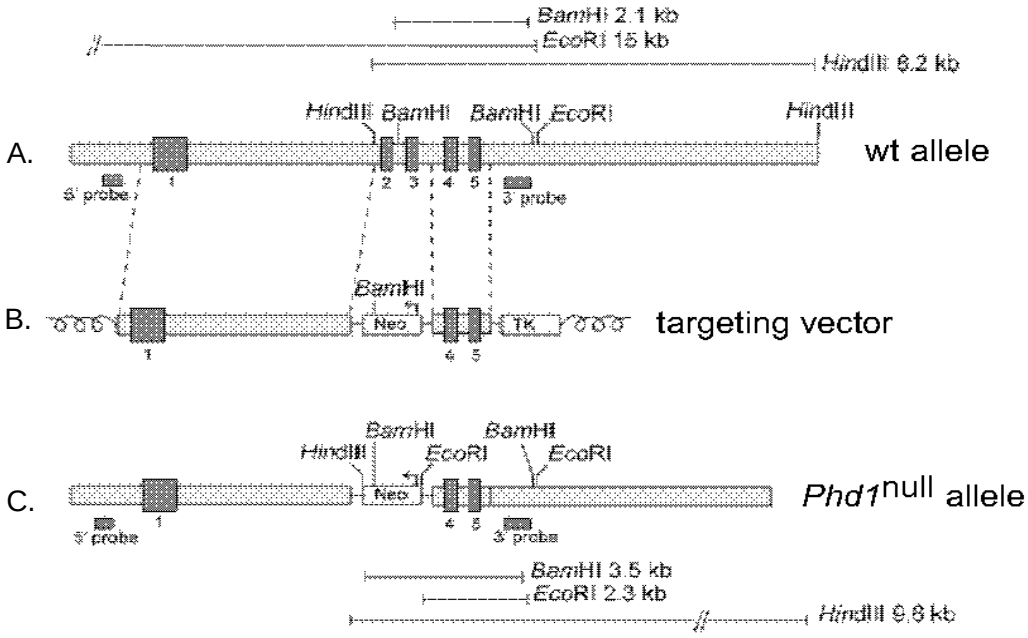

Figure 3: Generation of Phd1$^{-/-}$ mice. *Figure taken from Aragonés et al., 2008.* ***A:*** *Wild type (wt) Phd1 allele.* ***B:*** *schematic of the targeting vector used to generate Phd1 knockouts. A neomycin cassette (Neo) flanked by regions homologous to the wild type gene was used to knockout the central two exons of Phd1. A thymidine kinase (TK) gene outside of the homologous section was used to allow selection against random insertion events.* ***C:*** *After homologous recombination of the wild type allele and the targeting vector a Phd1^{-} allele was generated. Note, the numbering of the exons in this figure does not correlate with the real allele; one exon is missing from the image. So the neo cassette in the targeting vector replaces exons 3 and 4 instead of 2 and 3.*

Isolation of Liver Mitochondria

Mitochondria were isolated from wild type and *Phd1$^{-/-}$* livers of varying ages by differential centrifugation as described in Frezza et al.'s paper (2007) with a few deviations from the protocol. In brief the isolated livers were minced and immersed in isolation buffer at a ratio of 1:5-1:10 (w:v). This was then homogenized by 4-8 strokes of a Teflon pestle and transferred to a centrifuge tube. The homogenate was centrifuged for 10 minutes at 500g, supernatant transferred to a new tube and centrifuged for 10 minutes at 1000g; the

supernatant was spun at 13000g for a further 10 minutes. This resulted in a pellet of mitochondria which was washed in isolation buffer and centrifuged at 7000g for a further 10 minutes. The above was carried out at 4^{o}C or on ice.

Suspension in Detergent Buffers

The resulting mitochondria were quantified using the Pierce BCA kit (Thermo Scientific: PI-23221). The mitochondria were centrifuged for 10 minutes at 10,000g; remaining isolation buffer removed and the pellet resuspended in digitonin or dodecylmaltoside (DDM) buffer.

Ratios of DDM: mitochondria (g:g) or digitonin: mitochondria (g:g) varied (digitonin: mitochondria= 4:1 or 3:1; DDM: mitochondria= 0.5:1 or 1:1). The buffers were prepared using the NativePAGE sample Prep Kit (Invitrogen: BN2008) and 1µl protease inhibitor (Sigma: P8340) per 100µl buffer. The buffers were allowed to interact with the mitochondria for 20 minutes then they were centrifuged at 55000g for 15 minutes.

Blue Native Gel Electrophoresis (BNE)

NativePAGE sample additive (Invitrogen: BN2008) was added to 100µg of mitochondria and loaded onto a 4-16% Bis-Tris Polyacrylamide gel (Novex: BN2111BX10) alongside 7µl NativeMark unstained protein standard (Life Technologies; LC0725). NativePAGE running buffer (Novex: BN2001) was used

with 0.02% Coomassie Blue(NativePAGE Cathode Buffer Additive Invitrogen: BN2002) added to the cathode buffer until the sample moved a third down the gel then this was replaced with a cathode buffer consisting of 0.002% Coomassie. 1X NativePAGE running buffer was used as the anode buffer. Gels were run at 4^{o}C at 100V until the sample entered the gel then it was turned up to 300V. Gels were washed in dH_2O and stained with SimplyBlue (Invitrogen: LC6060).

Mass Spectrometry

Bands corresponding to known molecular weights of respiratory complexes I-V were cut from a BNE gel and sent for mass spectrometry to determine all proteins present in each band. The MitoMiner programme (Smith et al., 2012) was used to analyse the results.

High Resolution Clear Native Electrophoresis (hrCNE)

Clear Native electrophoresis was used to separate the above samples as of a previously described protocol (Wittig et al., 2007). Briefly 100µg of mitochondria or 7µl NativeMark protein standard was loaded into a NativePAGE 4-16% Bis-Tris Polyacrylamide gel (Novex: BN2111BX10). Digitonin samples were separated using a cathode buffer consisting of 1XNativePAGE running buffer (Novex: BN2001) with 0.05% sodium deoxycholate (DOC) and 0.01% DDM whereas DDM samples had 0.02% DDM in this mix. The anode buffer remained constant as 1X NativePAGE buffer. The gels were run at 100V until the sample entered the gel then it was turned up to 300V. hrCNE was performed in 4^{o}C for 3.5 hours.

In Gel Catalytic Activity Assays

After hrCNE the lanes were cut out the gel and in gel catalytic activity assays for mitochondrial complexes I-IV performed. This has been previously described (Wittig et al., 2007) with complex I and II assays performed on the same gel strip. Complex I buffer: 2.5mg/ml NitroBlue Tetrazolium (NTB)(Fisher Bioreagents: BP108-1); 0.1mg/ml β-nicotinamide adenine dinucleotide reduced dipotassium salt (NADH) (Sigma N4505), in 5mM Tris/HCl. Complex II buffer: 2.5mg/ml NTB, 200µl IM sodium succinate, 8µl 250mM phenezine methosulfate in 5mM Tris/HCl. Complex III buffer: 0.5mg/ml DAB in 50mM sodium phosphate. Complex IV buffer: 0.5mg/ml DAB and 1mg/ml cytochrome c powder in 50mM sodium phosphate. Gels were fixed in a solution of 10% acetic acid, 50% methanol and then washed in dH_2O. The protein standard and neighbouring samples were incubated in SimplyBlue stain (Invitrogen: LC6060) for 1 hour then washed in dH_2O.

The ImageJ programme (Schneider et al., 2012) was used to determine the intensities of each band form the activity assays. These were then normalised to the intensity of the corresponding band on the blue native gel and shown relative to the wild type control.

Western Blot

For each sample 20µg was boiled at 100^{o}C for 10 minutes in Laemmli sample buffer (Sigma: S3401-IVL). These were then loaded onto a 12% Tris-SDS acrylamide gel alongside 5µl Amersham Full-range rainbow molecular weight

marker (GE Healthcare: RPN800E). The gel was run at 150V in Tris/Glycine/SDS running buffer (Geneflow: B9-0032). Transfer to the nitrocellulose membrane was carried out using the wet transfer method for 1 hour at 100V. The gel was incubated in Quick blue Coomassie stain (triple red) overnight at room temp to stain for all remaining proteins on the gel and the nitrocellulose membranes blocked for an hour in 5% non-fat milk in PBST and incubated with the primary antibody UCP2 (Santa Cruz: Sc6526) at 1:500 dilution overnight at 4^{o}C. The primary antibody was washed off and the secondary antibody (Donkey Anti-goat Santa Cruz: Sc-2020 at 1:2000) allowed to bind for 1 hour at room temperature. This was then washed and visualised using the Amersham ECL detection kit (GE Healthcare: RPN2232).

ImageJ was used to determine the intensities of each UCP2 band. This was normalised to the intensity of the whole of the corresponding lane on the Coomassie stained gel and shown relative to the wild type band.

Results

Genotyping

The construct used to generate *Phd1*$^{-/-}$ mice has been described previously (Aragonés et al., 2008). It entails using a neomycin cassette to replace two exons of the wild type gene. Therefore in order to genotype the offspring PCR was performed using two sets of primers; one pair flanking the neomycin cassette and one pair against one of the missing exons. Figure 4A shows an example of how the genotyping was done; the homozygous knockout mice used in this project had been genotyped prior to the start. In the example litter shown, the parental cross was between a *Phd1*$^{+/+}$ mouse and a *Phd1*$^{+/-}$ so no *Phd1*$^{-/-}$ are present in the litter. Pups 1-10 and 13 are all wild type as they only produce bands when primers flanking exon 4 are used. Pups 11, 12 and 14 however are heterozygous as they produce bands for both primer pairs.

DDM versus Digitonin

Wild type mouse livers were used to refine the experimental procedure. The mitochondrial extraction procedure is based on a series of centrifugation steps that allows for the isolation of a fraction rich in mitochondria (Frezza et al., 2007). This was resuspended in detergent buffer to solubilise the mitochondria prior to native gel electrophoresis. Two buffers are commonly used in this procedure; digitonin and dodecylmaltoside (DDM) (Wittig et al., 2007). In this project both buffers were used. Digitonin is one of the mildest known detergents so supramolecular associations of multiprotein complexes were not disrupted (Wittig

et al., 2007) (Figure 4B). After clear native gel electrophoresis in gel catalytic assays were performed for respiratory complexes I-IV, this provides a semi-quantitative means of determining the ability of each complex to function. When solubilised in digitonin buffer complexes I, II and IV were isolated individually but additional bands were seen on the complex I gel: these represent supercomplexes where complex I is found in association with complex III and/or IV (Schagger and Pfeiffer, 2000). DDM is a mild non-ionic detergent which was able to isolate complexes I-IV individually (Figure 4C). When mitochondria were solubilised in DDM the activity of complex III can be determined (Figure 4C). This was not the case for digitonin buffer (Figure 4B). However DDM cannot maintain some of the protein-protein interactions between the individual respiratory complexes that link them together as supercomplexes. Therefore in order to get the most accurate view on the organisation and activity of the respiratory complexes both DDM and digitonin detergents were used to solubilise the isolated mitochondria.

Using wild type mouse liver mitochondria, different ratios of each buffer was used to try to determine which yields the clearest results. For digitionin buffer the ratios of detergent: mitochondria (g:g) used were 2:1, 3:1 and 4:1. Both 3:1 and 4:1 ratios provided clear results on the activity of each complex examined (Figure 4B). However the 4:1 ratio shows an additional faint band in the complex IV gel confirming its presence in the supercomplexes (Figure 4B). Therefore a ratio of 4:1 digitonin: mitochondria was used in this project. DDM: mitochondria ratios examined were 0.5:1 and 1:1 (Figure 4C). The results did not vary greatly between the two concentrations so a ratio of 1:1 DDM: mitochondria was used.

Blue Native Gel Electrophoresis (BNE)

Mitochondria solubilised in DDM or digitonin buffer were separated using blue native gel electrophoresis (BNE). This technique uses Coomassie dye in the cathode buffer and added directly to the samples to impose a charge shift in all proteins in the sample so that they all migrate to the anode. The BNE gels highlight two things; firstly it clearly shows that digitonin buffer was the only one able to isolate the supercomplexes as more bands were apparent in this detergent; secondly it shows that there is little to no difference in the size of each complex between the pairs of mice (Figure 4D). Each BNE shows the results of mitochondrial isolated from four separate pairs of age and sex matched mice; one *Phd1*$^{-/-}$ and one wild type sib. In both buffers the bands on the BNE were matched for each pair suggesting that any differences in activity found in the activity gels was not due to differences in the protein levels between matched samples (Figure 4D).

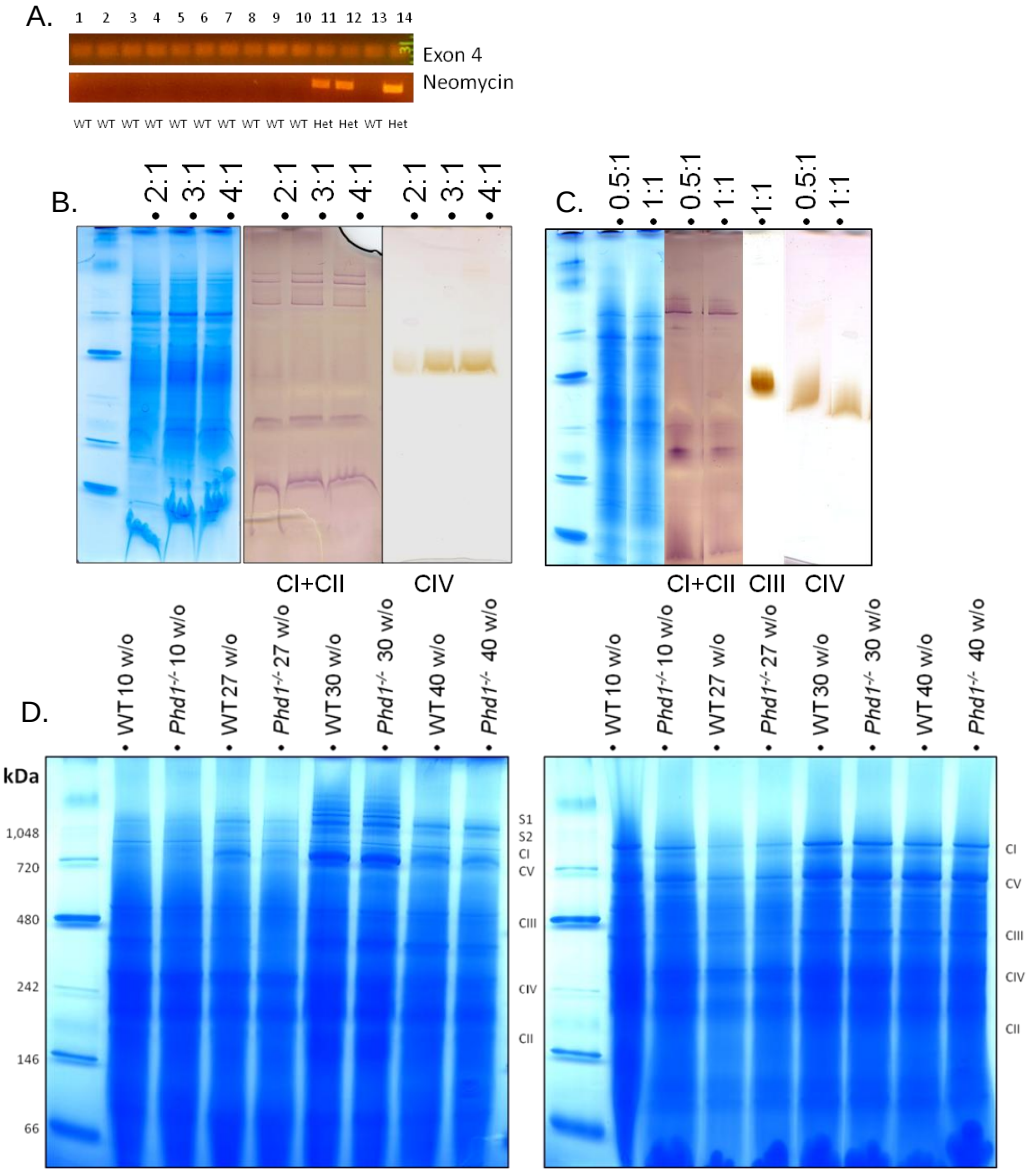

Figure 4: Refining the Experimental Procedure. A: *example of genotyping results. DNA was extracted from offspring of a Phd1$^{-/+}$ X Phd1$^{+/+}$ cross. Two PCRs were performed, one for the native exon 4 and the other for the knocked in neomycin cassette. Pups 11, 12 and 14 are Phd1$^{+/-}$ (Het), the rest are Phd1$^{+/+}$(wt). PCR products were electrophoresised on a 1.5% (neo) or 2% (exon 4) agarose gel.* ***B-D:*** *After isolation mitochondria were solubilised in DDM or digitonin buffer. These were then separated on a 4-16% Bis-Tris gel at 300V for 3.5hours.* ***B****: Mitochondria were resuspended in digitonin buffer at ratios of 2:1, 3:1, 4:1 digitonin: mitochondria (g/g). Clear native gel electrophesis was performed using a cathode buffer containing 0.01%DDM and 0.05%DOC. In gel catalytic activity assays were performed on resulting gel strips. Complex I and II assays were performed sequentially on the same gel strip. In order the bands in the CI+CII gel represent: supercomplexes I+II; complex I; then complex II.* ***C:*** *Isolated mitochondria were solubilised in DDM buffer at a ratio of 0.5:1 or 1:1 DDM: mitochondria (g/g). hrCNE was performed using a cathode buffer containing 0.02% DDM and 0.05% DOC.* ***D****: Mitochondria from wild type and Phd1$^{-/-}$ mice were solubilised in 4:1 digitonin (left) or 1:1 DDM (right) buffers. 100µg was loaded onto a gel and run using a cathode buffer containing 0.02% Coomassie dye that was replaced with 0.002% Coomassie after the sample had moved through a third of the gel. Resulting gels were washed in SimplyBlue stain for 1hr then in dH$_2$O overnight. w/o: weeks old. SI: supercomplex I, CI: complex I, CII: complex II, CIII: complex III, CIV: complex IV, CV: complex V. 7µl NativeMark Protein Standard (life technologies) wass loaded alongside the samples in all gels.*

Phd1 Knockout Causes a Reduction in The Activity of Respiratory Complex I, II and IV.

Mitochondria were isolated from the livers of a 27 week old female *Phd1*$^{-/-}$ mouse and an age and sex matched wild type sib. These were then solubilised in 4:1 digitonin buffer and run on a clear native gel. In gel catalytic activity assays were performed for complexes I-IV on the resulting gel strips. Incubation in complex III buffer provided no results, as was seen in the wild type digitonin practice gels. Complex I and IV buffers however presented clear differences in the activity of each complex in *Phd1*$^{-/-}$ mitochondria (Figure 5A). The activity of complex IV was almost completely abolished in the knockout mice. The complex I results show a similarly striking reduction in activity. Complex II isn't so visibly affected by loss of Phd1 (Figure 5A).

In order to quantify the data ImageJ was used to determine the intensities of each band. The results are shown here in two different forms. For every sample 100µg of protein was loaded into the well. Therefore the results are first shown as the intensity of the *Phd1*$^{-/-}$ activity relative to the wild type control (Figure 5B). In addition to this the results are normalised to the corresponding band from the BNE to account for errors in calculating protein concentration (Figure 5C). These results are shown as a fold change from the wild type sib. Both gels show the same pattern of activity, although the reduction in complex II activity is only visible when the results were normalised to the BNE. The activity of complex I is down by 75% in *Phd1*$^{-/-}$, complex II is reduced by almost 20% and complex IV by over 95% (Figure 5C).

DDM Buffer Alters the Activity of Respiratory Complexes I and IV from Phd1 Knockout Mouse Mitochondria.

Mitochondria from the same 27 week old female mice were solubilised in DDM buffer. These were separated by clear native gel electrophoresis and in gel catalytic activity assays for mitochondrial complexes I-IV performed. Interestingly when solubilised in DDM buffer *Phd1*$^{-/-}$ mitochondria did not show the same reduction in complex I, II and IV activity as was found in the digitonin buffer (Figure 5A-5C). Instead the activity of each complex was either unaffected or increased in *Phd1*$^{-/-}$ mitochondria with the intensity of the band representing complex II being considerably stronger in the *Phd1*$^{-/-}$ mitochondria (Figures 5D-F). This may be due to an error in the experimental procedure or may be a direct effect of the detergents.

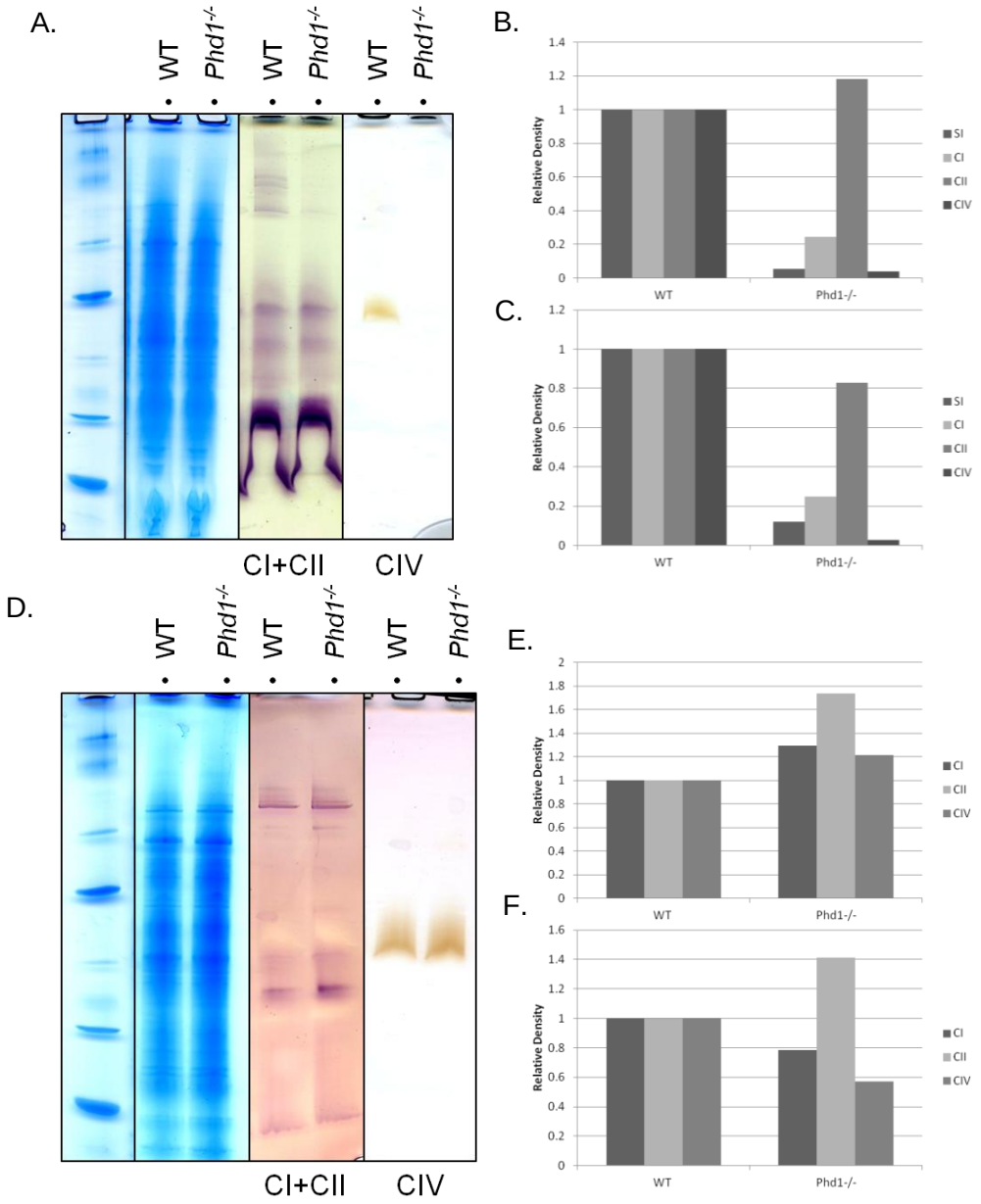

Figure 5: Loss of PHD1 Causes a Reduction in the Activity of Respiratory Complexes I, II and IV in 27 Week Old Female Mice. A*: Mitochondria from a Phd1$^{-/-}$ 27 week old female mouse and an age/sex matched wild type sib were solubilised in 4:1 digitonin: mitochondria buffer. 100µg was loaded onto a 4-16% Bis-Tris acrylamide gel and electrophoresis was performed using 0.01% DDM and 0.05% DOC cathode buffer. In gel activity assays were preformed for complex I, II and IV. The NativeMark protein standard and neighbouring lanes were incubated in SimplyBlue stain. A single gel strip shows complex I and complex II activity. In order the bands show, supercomplex I +II, complex I and then complex II at the bottom.* ***B-C:*** *ImageJ data from gels in* ***A****.* ***B:*** *Intensity of the bands is shown relative to the wild type control.* ***C:*** *Results from* ***B*** *are normalised against the corresponding band on the BNE gel (Figure 4D).* ***D:*** *Mitochondria from the same 27 week old female mice were solubilised in 1:1 DDM buffer. hrCNE was performed using 0.02%DDM in the cathode buffer. Gel strips were incubated in complex I-IV buffers. Complex III buffer yeilded no results. Complex I+II assays were preformed on the same strip sequentially.* ***E-F****: ImageJ was used to calculate the intensity of bands from* ***D.*** ***E:*** *The density of each band is shown relative to the wild type control.* ***F:*** *Results from* ***E*** *are normalised to the corresponding band from the BNE gel (Figure 4D).*

Phd1 Knockout May Reduce Respiratory Complex Activity More in Aged Mice.

It is well documented that deterioration of mitochondria is linked to the aging process (Wei et al., 2008). As mentioned previously the mice used so far in this project were 27 weeks old so the severity of the phenotype observed may be due to the age of the mice. Therefore mitochondria from a 10 week old female *Phd1*$^{-/-}$ mouse and an age and sex matched wild type sib were isolated. These were solubilised in digitonin buffer, separated on a clear native gel and complex I, II and IV activity assays performed on the resulting gel strips. In this pair of mice the activity of complex I was unaffected by loss of PHD1 (Figure 6A). As before the activity of complex IV was reduced in the mutant, however in the 10 week old mice the reduction in activity was less than 25% of the wild type whereas the 27 week old mice saw a reduction in activity of over 95% (Figure 6A-C). The activity of complex II in the knockout mouse mitochondria was only 27% of that of the wild type control (Figure 6C). This is much less than the activity of complex II in mitochondria from the 27 week old *Phd1*$^{-/-}$ mouse (Figure 4C). These results suggest that the age of the mice does affect the severity of mitochondrial decline in *Phd1*$^{-/-}$ mice.

Again when solubilised in DDM buffer the results differed to those found in digitonin buffer. Complex I and IV showed a greater decrease in activity in DDM buffer than they did in digitonin buffer whereas the decrease in complex II activity was less (Figure 6A-C). Complex III activity is only visible when mitochondria are solubilised in DDM buffer and these results showed that loss of PHD1 causes a decrease in activity of over 80% in 10 week old mice (Figure 6D-F).

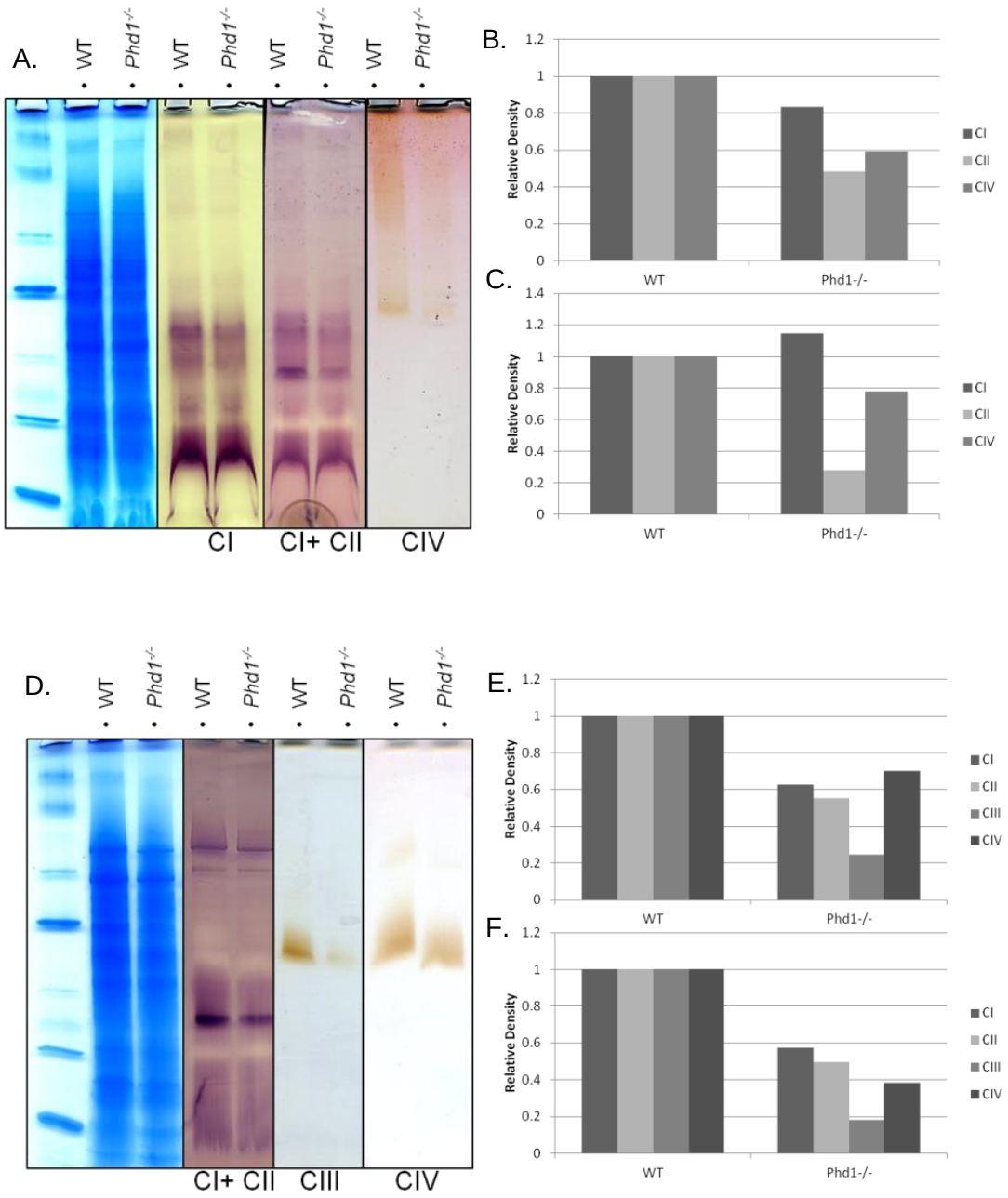

Figure 6: Age May Alter the Respiratory Phenotype of Phd1 Knockout Mitochondria. A, D: *Mitochondria were isolated from a 10 week old female Phd1$^{-/-}$ mouse and an age and sex matched wild type sib. These were solubilised in digitonin buffer at a ratio of 4:1 digitonin: mitochondria (**A**) or DDM buffer at a ratio of 1:1 (**D**). 100µg of each sample was loaded onto a 4-16% Bis-Tris gel and hrCNE performed using 0.01% (**A**) or 0.02% (**B**) DDM and 0.05% DOC in the cathode buffer. Enzyme activity assays specific for complexes I-IV were preformed on the resulting gel strips. NativeMark protein standard and neighbouring strips were incubated in SimplyBlue stain for 1hour. **B-C**: The intensity of each of the bands from **A** were calculated using ImageJ. **B:** Density is shown relative to wild type sib. **C:** Data from **B** was normalised to the density of the corresponding band in the BNE (Figure 4D). **E-F:** relative intensities of bands from **D. E:** ImageJ was used to determine density of each band relative to the corresponding wild type sib. **F**: Data from **E** was normalised to the corresponding band of the BNE (fig).*

Phd1 Knockout May Have Sex Specific Effects.

PHD1 is a target of the oestrogen receptor so the protein may have sex specific roles and the effect of Phd1 knockout may differ between the sexes (Seth et al., 2002). The previous mice examined were female therefore mitochondria from a 40 week old *Phd1*$^{-/-}$ male mouse and an age and sex matched wild type sib were isolated. These were solubilised in digitonin buffer, separated by CNE and complex I, II and IV activity assays performed. Unlike previous results the activity of all complexes appeared to increase by 20% or more in the mutant mice (Figure 7A-C). Similarly when solubilised in DDM buffer the activity of complexes I- IV was either unaffected by the loss of PHD1 or increased with it (Figure 7D-F). These results suggest that the decline in respiratory complex activity observed in *Phd1*$^{-/-}$ mice is specific to females.

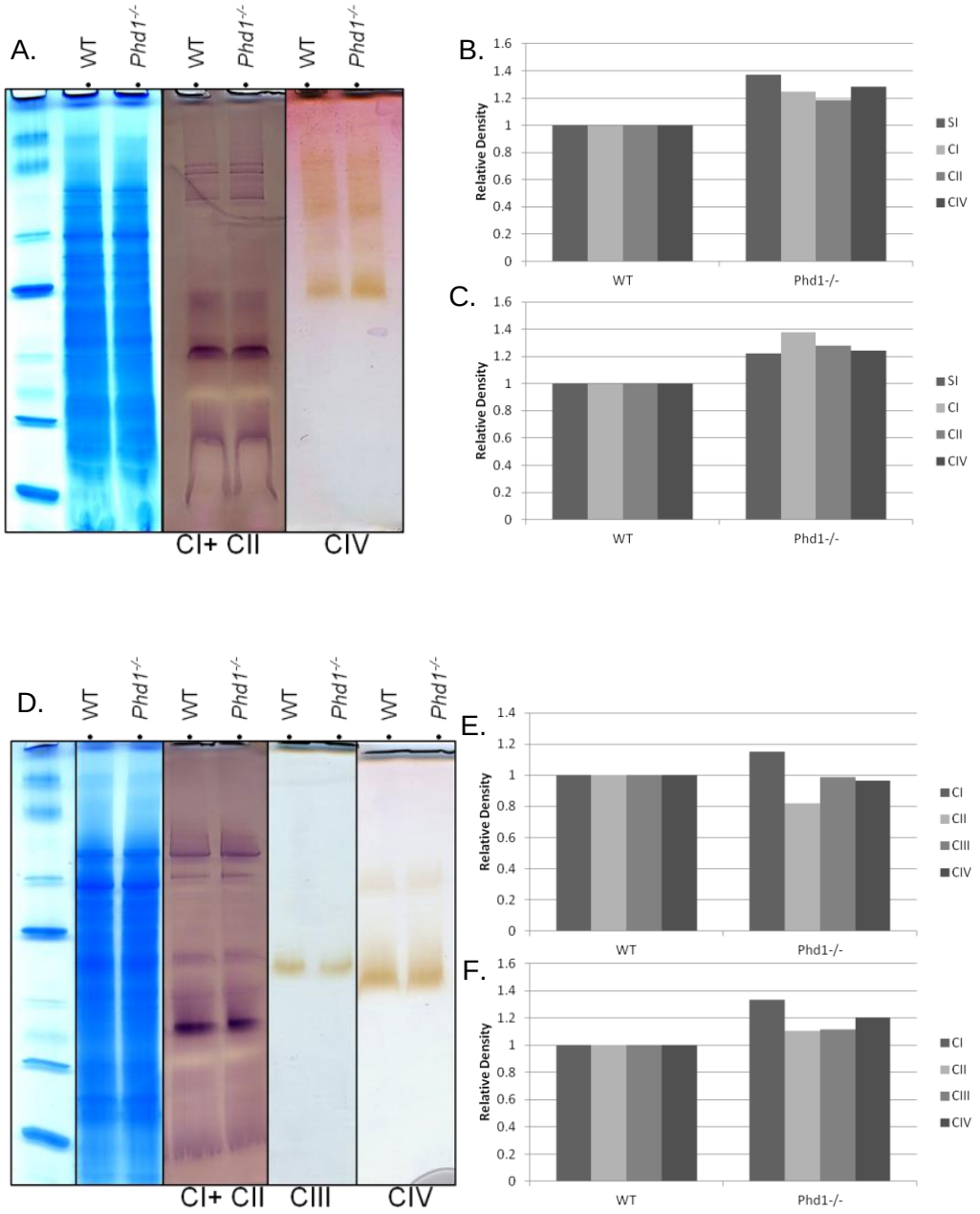

Figure 7: Knockout of Phd1 May Have Sex Specific Effects. A, D*: Mitochondria from a 40 week old male Phd1$^{-/-}$ mouse and an age and sex matched wild type sib were solubilised in 4:1 digitonin buffer (**A**) or 1:1 DDM buffer (**D**). 100µg mitochondria was loaded onto a 4-16% Bis-Tris gel and hrCNE performed using a cathode buffer containing 0.01% (**A**) or 0.02% (**D**) DDM and 0.05% DOC. Activity assays for complexes I-IV were preformed on the resulting gel strips. NativeMark Protein Standard and neighbouring lanes were incubated in SimplyBlue stain for 1hour. **B-C**: Relative density of bands from **A. B:** ImageJ was used to determine the intensity of each band from **A**, Phd1$^{-/-}$ bands are shown relative to the wild type control. **C:** results from **B** are normalised to the corresponding band in the BNE (Figure 4D). **E-F:** Relative density of activity assays from **D. E:** Density of bands from **D** are shown relative to the wild type sib. **F**: Results from **E** are normalised to the density of the corresponding bands in the BNE (Figure 4D).*

Loss of PHD1 has a Variable Effect on the Activity of Complexes I-IV.

Mitochondria were isolated from two more *Phd1*$^{-/-}$ female mice of about 30 weeks old and two wild type sibs. These mice resembled the initial pair in both age and sex. However the results of the in gel activity assays do not match (Figure 8A, E). In one pair loss of PHD1 increased complex I activity, specifically when found in the supercomplex (Figure 8A). The activity of complex II was unaffected and complex IV activity decreased by less than 10% when solubilised in digitonin buffer (Figure 8A). Only the activity of complex III is shown in DDM buffer as this cannot be seen when the mitochondria are solubilised in digitonin. Complex III activity was reduced by almost 75% in the *Phd1*$^{-/-}$ mouse (Figure 8A-D). In the other pair complex IV activity was reduced by 67% in the *Phd1*$^{-/-}$ mitochondria but the activity of all the other complexes was increased with complex III activity being over two fold higher in the mutant (Figure 8E-H). These results show that there is huge variability in the effects of PHD1 loss on mitochondrial complex activity. The results for all 30 week female mice were combined and show that the general trend of PHD1 loss is a reduction in the activity of complex I by about 15% and complex IV by almost 60% (Figures 8I-J). In this figure, complex II appears unaffected and complex III activity increased in the mutant. However the complex III result is due to a single pair of 30 week old mice which showed a huge increase in activity in the mutant (Figure 8F-H).

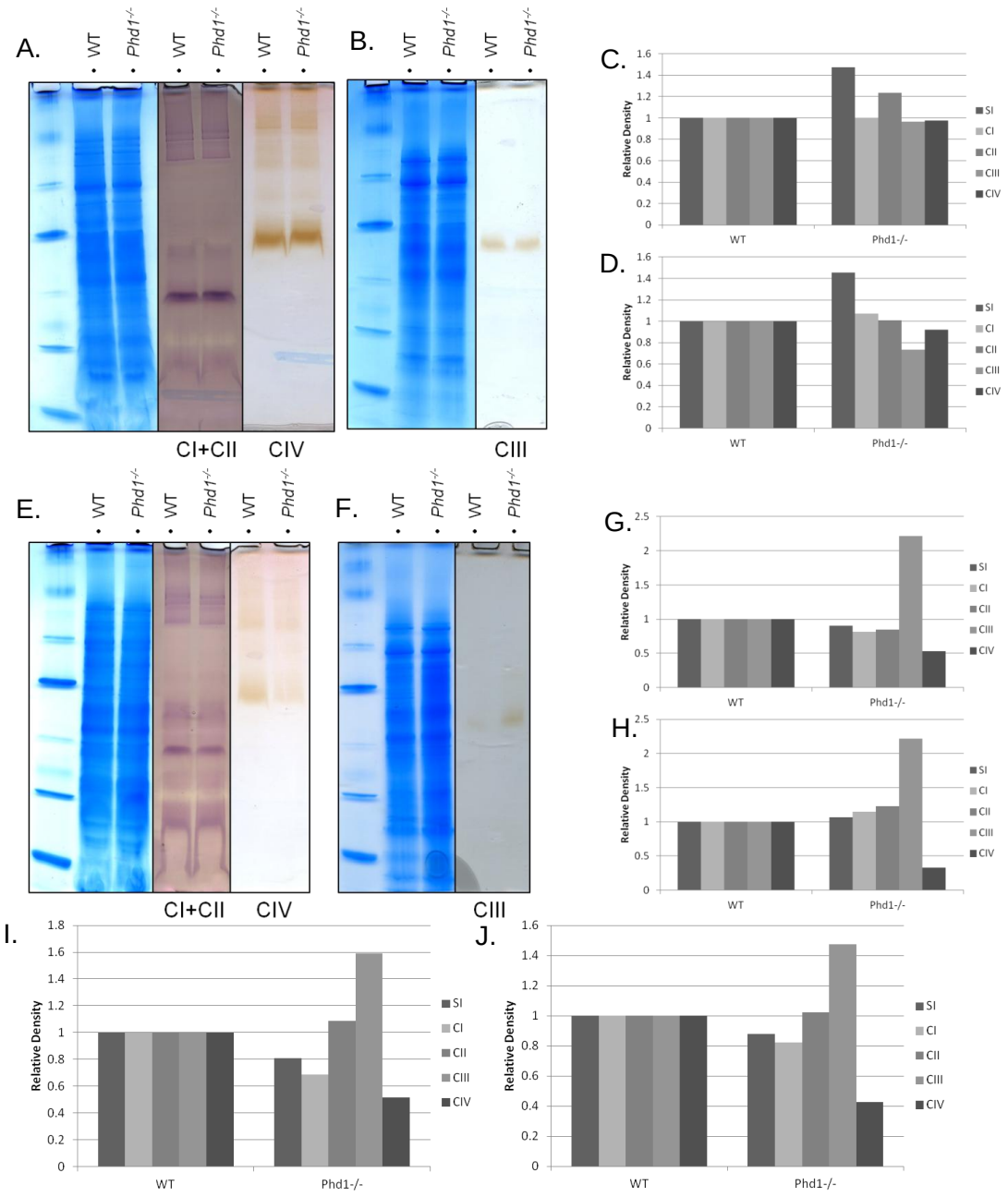

Figure 8: The Effect of PHD1 Knockout on Respiratory Complexes Activity Varies*. **A, B, E, F:** Mitochondria were isolated from two 30 week old female Phd1$^{-/-}$ mice and two age and sex matched wild type sibs. **A-B** and **E-F** represent two independent experiments. Mitochondria were solubilised in 4:1 digitonin (**A, E**) or 1:1 DDM (**B, F**) and 100µg of each sample was loaded onto a 4-16% Bis-Tris gel. hrCNE was performed using a cathode buffer containing 0.01% (**A, E**) or 0.02% (**B,F**) DDM and 0.05% DOC. Enzyme activity assays were performed on resulting gel strips. NativeMark protein standard and neighbouring lanes were incubated in SimplyBlue stain for 1 hour. **C-D:** ImageJ was used to determine the relative density of bands from **A** and **B**. Complex I, II and IV data are from digitonin buffer (**A**), complex III data is from DDM buffer (**B**). **C:** Density is shown relative to wild type sib. **D:** Results from **C** are shown normalised to the corresponding BNE band (Figure 4D). **G-H:** Relative density of bands from **E** and **F. G**: ImageJ was used to determine the density of each band relative to the control. **H:** Results from **G** were normalised to the corresponding band on the BNE gel (Figure 4D). **I-J:** Average results for all three pairs 30 weeks old females. **I:** ImageJ was used to determine the density of bands for each activity assay. Phd1$^{-/-}$ results are shown relative to the wild type sib. **J:** Relative density of the bands from **I** was normalised to the corresponding band form the BNE gel (Figure 4D).*

Mitochondria from Phd1 Knockout Mouse Livers have Less UCP2.

The variability of the results lead to the hypothesis that respiratory complex decline is not a direct result of PHD1 loss. A potential explanation for this could be that *Phd1*$^{-/-}$ mitochondria produce more reactive oxygen species than wild type. These would indiscriminately damage proteins and DNA in the mitochondria. Therefore a UCP2 western was performed on the isolated mitochondria. UCP2 spans the inner mitochondrial membrane, controls the electrochemical potential of the membrane and as such can control the amount of ROS produced (Donadelli et al., 2013). In lieu of a stable mitochondria specific control gene the total protein content on the gel was determined by staining the gel with Coomassie and density of the UCP2 band was normalised to this (Figure 9B). The overall pattern was a reduction in UCP2 levels in the *Phd1*$^{-/-}$ mitochondria (Figure 9B). However mitochondria from the male mouse had increased UCP2 levels in the Phd1 knockout and the reduction in UCP2 in the majority of the females was only between 5 and 10% (Figure 9B). A single 30 week female showed 75% less UCP2 in the *Phd1*$^{-/-}$ mitochondria than the wild type however this result did not correlate with that of the activity assays (Figure 8A).

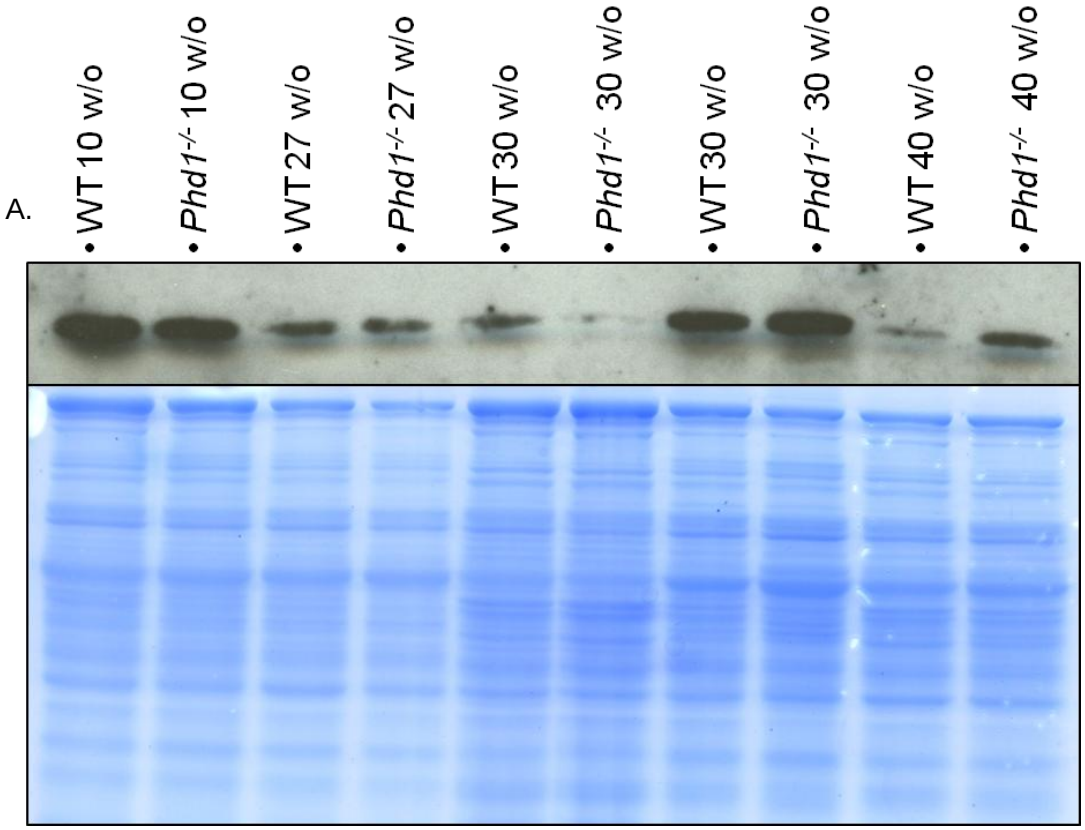

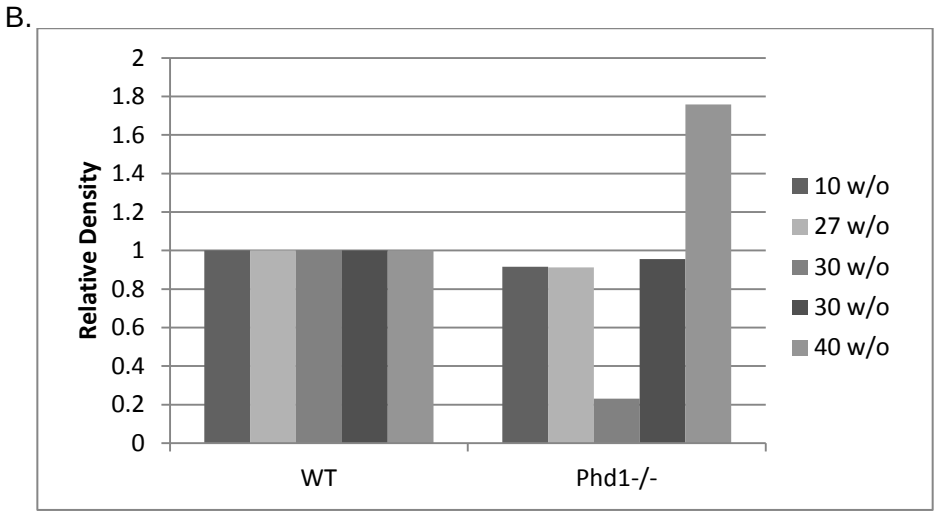

***Figure 9: UCP2 protein levels were reduced in Phd1$^{-/-}$ female mice**. **A:** 20µg of mitochondria solubilised in digitonin buffer was loaded onto an SDS gel and a western blott for UCP2 performed (top). After blotting the remaining proteins in the gel were stained using Coomassie blue (bottom). **B**: ImageJ data shows insensity of UCP2 band normalised to that of the blue gel. Phd1$^{-/-}$ data is shown relative to the corresponding wild type sib. Results are combined from two independent experiments. w/o= weeks old.*

Mass Spectrometry Confirms Reduced Function of Complex I in 27 Week Old Phd1$^{-/-}$ Mitochondria.

Blue native gel electrophoresis was performed using 100µg of mitochondria isolated from the 27 week old female mice discussed previously. Bands corresponding to respiratory complexes I-V were excised from the gel using published molecular weights as a guideline (Wittig et al., 2006). Mass spectrometry was performed to determine all proteins present in each band. Analysis of the bands from complexes II, III and IV suggests that the wrong bands were excised as the presence of the relevant subunits in each band was minimal. However complex I bands were rich in NADH dehydrogenase subunits and complex V bands rich in ATP synthase subunits suggesting that these bands were correct. The MRC MitoMiner programme was used to analyse the results (Smith et al., 2012). All bands were enriched for mitochondrial proteins, however proteins from peroxisomes and the endoplasmic reticulum were also present showing that although differential centrifugation produces a fraction rich in mitochondria it does not completely eliminate contamination by other organelles.

The MitoMiner programme was used to determine which UniProt keywords were enriched in each sample (Smith et al., 2012). Along with showing which organelles are present this gives an indication of the biological processes carried out by the proteins in the sample. The top 12 results are shown in Table 1. Irrelevant keywords such as those from organelles other than mitochondria were removed. The table shows the p-values for enrichment of the *Phd1*$^{-/-}$ and wild type samples against the default background population calculated by the MitoMiner programme using hypergeometric distribution. For complex I p-values for oxidoreductase and

NAD are lower in the mutant than the wild type. This indicates that there are fewer proteins involved in the transferral of electrons to/from NAD(H) in the *Phd1*$^{-/-}$ sample. As the function of complex I is to transfer electrons from NADH to ubiquinone this is consistent with the 75% reduction in complex I activity seen in the activity assays (Figure 5C). Interestingly the complex V results show that the p-value for ATP synthesis in the *Phd1*$^{-/-}$ sample is lower than that of the wild type suggesting that ATP production in the knockout is higher than normal (Table 1B).

Consistent across both complex I and complex V samples is the fact that proteins involved in fatty acid and lipid metabolism are less enriched in *Phd1*$^{-/-}$ than wild type samples (Tables 1A-B). This is interesting as the livers of *Phd1*$^{-/-}$ appeared to be less fatty than their wild type counterparts. Additionally there is an increase in H+ ion transport in the *Phd1*$^{-/-}$ samples (Tables 1A-B). Previous results have shown reduced activity of complexes I and IV and reduced levels of UCP2 in these mitochondria both of which would suggest less H+ transport. The mass spectrometry results therefore might suggest that the complex I subunits damaged in the *Phd1*$^{-/-}$ mitochondria are those involved in the reduction of NADH not the transport of H+ ions across the inner mitochondrial membrane.

Complex I

UniProt Keyword	WT	*Phd1-/-*
Mitochondrion	1.12E-99	2.34E-64
Acetylation	4.65E-85	2.55E-52
Transit peptide	1.33E-72	2.93E-43
Mitochondrion inner membrane	3.44E-68	4.96E-56
Respiratory chain	3.52E-55	4.72E-51
Electron transport	1.01E-48	7.10E-48
Oxidoreductase	3.95E-36	1.11E-12
Transport	4.57E-27	1.07E-27
Fatty acid metabolism	1.50E-22	9.96E-03
Lipid metabolism	2.68E-18	4.46E-02
Hydrogen ion transport	3.18E-16	1.55E-19
NAD	6.42E-16	2.23E-07

Complex V

UniProt Keywords	WT	*Phd1-/-*
Mitochondrion	2.14E-54	6.04E-44
Acetylation	2.06E-48	2.61E-47
Transit peptide	8.26E-48	8.76E-39
Oxidoreductase	2.55E-25	1.06E-18
Mitochondrion inner membrane	3.38E-25	2.44E-27
Fatty acid metabolism	2.06E-19	1.59E-14
Lipid metabolism	3.54E-19	1.67E-15
Hydrogen ion transport	6.87E-15	4.11E-17
ATP synthesis	5.03E-14	9.94E-17
CF(0)	1.37E-12	9.97E-13
Monooxygenase	5.79E-09	8.44E-03
NADP	7.49E-09	4.17524E-05

Table 1: Differential Enrichment in WT and Phd1$^{-/-}$ Mass Spectrometry Samples. *Mitochondria from 27 week Phd1$^{-/-}$ female mouse and age and sex matched wild type sib were solubilised in DDM buffer, separated by BNE and the bands corresponding to each complex in the respiratory chain excised and sent for mass spectrometry. The MitoMiner programme was used to look for UniProt keywords enriched in the resulting data. Tables show the top 12 results for complex I (left) and V (right). Keywords unrelated to mitochondria were removed from the data. The numbers shown are the p-values calculated by MitoMiner using hypergeometric distribution to determine which UniProt keywords were enriched in the proteins present in the wild type and Phd1$^{-/-}$ samples.*

Discussion

In normoxia the PHD proteins control the degradation of HIF-α by hydroxylating specific residues which allows for the VHL protein to bind and ubiquitinate (Papandreou et al., 2006; Bruik and McKnight, 2001). This process is oxygen dependent. In the absence of oxygen PHDs cannot hydroxylate HIF so VHL cannot bind and HIF-α can dimerize with HIF-β and control the hypoxia response. HIF-α is constitutively expressed so this mechanism provides a quick means of responding to drops in oxygen concentration (Applehoff et al., 2004). The active HIF dimer induces the expression of genes involved in erythropoiesis and angiogenesis and brings about a change in basal metabolism so that less oxygen is consumed (Papandreou et al., 2006). Evidence is starting to suggest that the PHD proteins may also have roles outside of HIF-α control (Appelhoff et al., 2004; Zhang et al., 2009; Cummins et al., 2006; Moser et al., 2013) .PHD1 has been linked to regulation of cyclin DI, NF-kB and Cep192 levels in processes completely independent of HIF (Zhang et al., 2009; Cummins et al., 2006; Moser et al., 2013).

The vast majority of cellular ATP is produced in the mitochondria (Mailloux et al., 2013). Glycolysis occurs in the cytosol and in normoxia most glycolytic intermediates are passed to the matrix of the mitochondria where the TCA cycle occurs. This produces the NADH required to fuel the electron transport chain (Mailloux et al., 2013). Complexes I-IV of the electron transport chain carry out a series of redox reactions transferring electrons from the initial electron donor; NADH to the final acceptor; oxygen (Wei et al., 2009; Mailloux et al., 2013)

Complexes I, III and IV all span the tightly controlled inner mitochondrial membrane and they use the energy produced from this transfer of electrons to transport hydrogen ions across the membrane to create a proton gradient (Wei et al., 2009). The gradient is a store of energy which is harnessed by complex V (ATP synthase) to produce ATP (Wei et al., 2009; Davis and Williams, 2012). This process requires oxygen so in hypoxia the HIF proteins regulate a shift in metabolism so that more ATP is produced by glycolysis and less oxygen is consumed by the mitochondria (Papandreou et al., 2006). PDK1 is induced by HIF-1 causing a reduction in PDC activity (Papandreou et al., 2006). PDC controls the conversion of pyruvate to acetyl CoA so this means reduced entry of glycolytic intermediates into the TCA cycle and increased glycolysis during hypoxia (Papandreou et al., 2006). Aragonés et al. (2008) found a similar process was occurring in the skeletal muscle of mice lacking PHD1. They proposed that this occurred through HIF-2α and protected the muscle against ischemia (Aragonés et al., 2008). A similar result was observed in *Phd1*$^{-/-}$ mouse livers (Schneider et al., 2010). This project aimed to expand upon these findings and examine the respiratory phenotype of mitochondria from *Phd1*$^{-/-}$ mouse livers.

Differential centrifugation was used to isolate mitochondria from the livers of *Phd1*$^{-/-}$ mice and an age and sex matched wild type sib. The resulting mitochondria were then solubilised in detergent buffer and separated by native gel electrophoresis. In gel catalytic activity assays specific to each of the four mitochondrial complexes were preformed to provide a semi-quantifiable means of determining differences in the ability of each complex to function in the mutant mice. The overall conclusion drawn from these experiments was that loss of Phd1

leads to a reduction in the activity of complexes I-IV. However this result varied greatly between the different pairs of mice used in terms of how much activity was lost in the mutant and which of the four complexes were affected (Figures 5-8).

The affect of age and sex on these results were considered. Mitochondrial decline is thought to be closely linked to aging (Wei et al., 2008). As cells age the ability to prevent ROS accumulation declines and that this damages the mitochondria (Wei et al., 2008). Therefore mitochondrial damage resulting from PHD1 loss may accumulate with age. The results showed that the activity of the respiratory complexes was less in a 27 week old *Phd1*$^{-/-}$ mouse than a corresponding 10 week old mouse (Figure 5-6). However this was not the case when a further two pairs of 30 week old mice were examined. Instead both *Phd1*$^{-/-}$ mice showed less mitochondrial damage than was seen in the 10 week old mouse (Figure 8A-H). Therefore we cannot conclude from these findings that the loss of complex activity in *Phd1*$^{-/-}$ mouse mitochondria increases with age. More young mice would need to be used in order to determine whether there is a correlation. As PHD1 is thought to be a direct target of the oestrogen receptor it may have sex specific functions (Seth et al., 2002). The 10-30 week old mice used in this project were all females. Therefore the activity of the respiratory complexes of mitochondria from a 40 week old male *Phd1*$^{-/-}$ mouse and an age and sex matched wild type sib were determined. Mitochondria from the male *Phd1*$^{-/-}$ mouse showed no loss of activity in complexes I-IV and instead a slight increase in activity was observed (Figure 7A-F). This would suggest that the affects of Phd1 knockout on the respiratory phenotype of mouse liver mitochondria is sex specific. However in order to confirm this theory the experiment would need to be repeated with more males.

Additionally matching the age of the males with the females would provide more accurate results.

This project has shown that loss of PHD1 causes extremely variable effects on the activity of mitochondrial complexes I-IV. This would suggest that the pathway from Phd1 knockout to mitochondrial damage is not a linear one. A promising hypothesis is that PHD1 loss causes an increase in the amount of reactive oxygen species produced within the cell. Mitochondria are prone to damage by ROS and as ROS are known to damage DNA and proteins indiscriminately the effects would vary with each mouse producing differences in the severity and location of the damage. This is in fitting with the variability of the results in this project. Therefore the levels of superoxide in *Phd1*$^{-/-}$ livers could be assessed for example by staining with the oxidative fluorescent dye dihydroethidine (Scortegagna et al., 2003). Additionally treating the mice with antioxidants and seeing whether wild type mitochondrial phenotype is restored would provide evidence that loss of respiratory complex activity in *Phd1*$^{-/-}$ mice is due to excess ROS production. However as ROS may have also damaged mtDNA functional decline in the respiratory complexes may not be completely restored by antioxidant treatment. Interestingly another facet of hypoxia signalling involves the inhibition of PHD proteins by excess ROS (Guzy and Schumacker, 2006). It is thought that in the initial stages of hypoxia mitochondria produce more ROS which target the Fe^{2+} ion required by the PHD proteins (Guzy and Schumacker, 2006). Therefore if Phd1 knockout leads to an increase in ROS this could in turn inhibit the function of the remaining PHDs.

ROS accumulation could be due to two things; either more ROS are being produced or the ability of antioxidants and ROS scavengers to control the levels of ROS are reduced. High mitochondrial membrane potential has been linked to increased ROS production (Korshunov et al., 1997). A Clarke-type electrode can be used to measure respiration in isolated mitochondria (Frezza et al., 2007). Coupled mitochondria should consume oxygen faster in the presence of ADP and this rate should increase when an uncoupler is added. This project aimed to use this technique to determine whether *Phd1*$^{-/-}$ mitochondria were more coupled than wild type and therefore have a higher membrane potential. However problems with the isolation procedure meant that the mitochondria isolated were not intact enough for this experiment. Therefore a UCP2 western was performed. UCP2 spans the inner mitochondrial membrane and can uncouple the membrane by allowing ions across (Donadelli et al., 2013). The western showed a general reduction in UCP2 in the *Phd1*$^{-/-}$ mitochondria however this was not consistent across all pairs of mice examined. In keeping with the theory that loss of PHD1 has sex specific affects the mitochondria from the 40 week old male mice showed an increase in UCP2 of over 75% (Figure 9A-B). The reduction in UCP2 levels seen in the females was generally only 5-10% with the results of a single 30 week old female being over 75% less UCP2 in the mutant (Figure 9A-B). However differences in these results do not correlate with those of the activity assays suggesting that loss of UCP2 is not the sole reason for mitochondrial damage in *Phd1*$^{-/-}$ mice.

In addition to the regulation of HIF-2α stability PHD1 has HIF-independent roles (Zhang et al., 2009; Cummins et al., 2006). Scortegagna et al. (2003) found an increase in the activity of complex II and complex IV in skeletal myofibres from

Hif-2α knockout mice. These results are consistent with those discussed in this project as the opposite effect was observed; complex II and IV activity was reduced in *Phd1*$^{-/-}$ mitochondria. Schneider et al. (2010) showed an increase in HIF-2α protein levels in *Phd1*$^{-/-}$ mice using the mouse model discussed in this project. Additionally the protection against hypoxia observed in *Phd1*$^{-/-}$ mice is partially lost upon addition of HIF-2α siRNA, suggesting that this is HIF-2α dependent (Schneider et al., 2010). However whether this increase in HIF-2α is sufficient to cause the increase in glycolytic production of ATP and decrease in oxygen consumption observed in *Phd1*$^{-/-}$ mice is not discussed (Schneider et al., 2010; Aragonés et al., 2008). Therefore the functional decline of respiratory complexes I-IV in *Phd1*$^{-/-}$ mice discussed in the current report may be due to the increased levels of HIF-2α previously seen in the mouse model used but more work needs to be done to determine whether this is the case (Schneider et al., 2010). Repeating the experiments with *Phd1*$^{-/-}$ mice crossed with *Hif-2α*$^{+/-}$ mice would be the first step in doing so.

Mass spectrometry was performed on bands corresponding to complexes I-V of the ETC from *Phd1*$^{-/-}$ mouse mitochondria. Unfortunately the results for complex II, III and IV suggested that the wrong bands were excised from the gel. Therefore this would need to be repeated, perhaps by using a protein stained strip from a hrCNE gel instead of that of a BNE gel. This way the complex activity assays could be performed alongside it and the relevant bands more easily determined. The complex I results showed a drop in enrichment in proteins involved in NAD and oxidoreductase which corresponds with the reduction in complex I activity shown in the in gel catalytic assays (Table1/Figure 5A). An increase in proteins involved hydrogen ion transport was observed in both the complex I and complex

V samples. This could provide a potential mechanism to explain the theory of excess ROS production in *Phd1*$^{-/-}$ mice as it may suggest a higher membrane potential at the inner mitochondrial membrane (Korchunovet al., 1997). However the transport of protons could go both ways and these results are that of a single mouse so more work is needed in order to prove this.

Conclusion

This project has shown that Phd1 knockout results in a decline in function of mitochondrial complexes I-IV. However this result varies considerably suggesting that a linear pathway from Phd1 loss to mitochondrial damage does not exist. A potential mechanism to explain this variability is through increased ROS production in the mutant which would damage mitochondrial proteins and DNA arbitrarily. More work needs to be done in order to prove this; first by repeating the experiment with more age and sex matched mice then determining whether *Phd1*$^{-/-}$ mice show increased levels of ROS. The results also suggest that the mitochondrial decline observed in *Phd1*$^{-/-}$ mice may be sex specific as the male mouse examined did not show the same pattern of mitochondrial complex activity loss found in the females.

Acknowledgments

With thanks to Dr Dan Tennant and Giulio Laurenti for all their help.

References:

Andreyev, A Y., Kushnareva, Y E., and Starkov, A A. “Mitochondrial Metabolism of Reactive Oxygen Species.” *Biochemistry. Biokhimiia* 70, no. 2 (February 2005): 200–214.

Appelhoff, R J., Tian, Y M., Raval, R R., Turley, H., Harris, A L., Pugh, C W., Ratcliffe, P J., and Gleadle, J M. “Differential Function of the Prolyl Hydroxylases PHD1, PHD2, and PHD3 in the Regulation of Hypoxia-Inducible Factor.” *Journal of Biological Chemistry* 279, no. 37 (September 10, 2004): 38458–65. doi:10.1074/jbc.M406026200.

Aragonés, J., Schneider M., Geyte, K V., Fraisl, P., Dresselaers, T., Mazzone, M., Dirkx, R., et al. “Deficiency or Inhibition of Oxygen Sensor Phd1 Induces Hypoxia Tolerance by Reprogramming Basal Metabolism.” *Nature Genetics* 40, no. 2 (February 2008): 170–80. doi:10.1038/ng.2007.62.

Bandy, B, and Davison, A J. “Mitochondrial Mutations May Increase Oxidative Stress: Implications for Carcinogenesis and Aging?” *Free Radical Biology & Medicine* 8, no. 6 (1990): 523–39.

Bruick, R K, and McKnight, S L. “A Conserved Family of Prolyl-4-Hydroxylases That Modify HIF.” *Science (New York, N.Y.)* 294, no. 5545 (November 9, 2001): 1337–40. doi:10.1126/science.1066373.

Cummins, E P., Berra, E., Comerford, K M., Ginouves, A., Fitzgerald, K T., Seeballuck, F., Godson, C., et al. “Prolyl Hydroxylase-1 Negatively Regulates IκB Kinase-B, Giving Insight into Hypoxia-Induced NFκB Activity.” *Proceedings of the National Academy of Sciences* 103, no. 48 (November 28, 2006): 18154–59. doi:10.1073/pnas.0602235103.

Davis, R E., and Williams, M. “Mitochondrial Function and Dysfunction: An Update.” *Journal of Pharmacology and Experimental Therapeutics* 342, no. 3 (September 1, 2012): 598–607. doi:10.1124/jpet.112.192104.

Donadelli, M., Dando, I., Fiorini, C., and Palmieri, M. “UCP2, a Mitochondrial Protein Regulated at Multiple Levels.” *Cellular and Molecular Life Sciences* 71, no. 7 (April 1, 2014): 1171–90. doi:10.1007/s00018-013-1407-0.

Fong, G-H., and Takeda, K. “Role and Regulation of Prolyl Hydroxylase Domain Proteins.” *Cell Death & Differentiation* 15, no. 4 (February 15, 2008): 635–41. doi:10.1038/cdd.2008.10.

Frezza, C, Cipolat, S., and Scorrano, L. “Organelle Isolation: Functional Mitochondria from Mouse Liver, Muscle and Cultured Filroblasts.” *Nature Protocols* 2, no. 2 (February 2007): 287–95. doi:10.1038/nprot.2006.478.

Guzy, R D., and Schumacker, P T., “Oxygen Sensing by Mitochondria at Complex III: The Paradox of Increased Reactive Oxygen Species during Hypoxia.” *Experimental*

Physiology 91, no. 5 (September 1, 2006): 807–19. doi:10.1113/expphysiol.2006.033506.

Harman, Denham. “Aging: A Theory Based on Free Radical and Radiation Chemistry.” *Journal of Gerontology* 11, no. 3 (July 1, 1956): 298–300. doi:10.1093/geronj/11.3.298.

Kaelin, W G. Jr, and Ratcliffe, P J., “Oxygen Sensing by Metazoans: The Central Role of the HIF Hydroxylase Pathway.” *Molecular Cell* 30, no. 4 (May 23, 2008): 393–402. doi:10.1016/j.molcel.2008.04.009.

Korshunov, S S., Skulachev, V P., and Starkov, A A. “High Protonic Potential Actuates a Mechanism of Production of Reactive Oxygen Species in Mitochondria.” *FEBS Letters* 416, no. 1 (October 13, 1997): 15–18.

Mailloux, R J, Jin, X., and Willmore, W G. “Redox Regulation of Mitochondrial Function with Emphasis on Cysteine Oxidation Reactions.” *Redox Biology* 2 (December 19, 2013): 123–39. doi:10.1016/j.redox.2013.12.011.

Mailloux, R J., and Harper, M-E. “Uncoupling Proteins and the Control of Mitochondrial Reactive Oxygen Species Production.” *Free Radical Biology and Medicine* 51, no. 6 (September 15, 2011): 1106–15. doi:10.1016/j.freeradbiomed.2011.06.022.

Metzen, E, Berchner-Pfannschmidt, U., Stengel, P., Marxsen, J H., Stolze, I., Klinger, M., Huang, W Q., et al. “Intracellular Localisation of Human HIF-1α Hydroxylases: Implications for Oxygen Sensing.” *Journal of Cell Science* 116, no. 7 (April 1, 2003): 1319–26. doi:10.1242/jcs.00318.

Moser, S C., Bensaddek, D., Ortmann, B., Maure, J-F., Mudie, S., Blow, J J., Lamond, A I., Swedlow, J R., and Rocha, S. “PHD1 Links Cell-Cycle Progression to Oxygen Sensing through Hydroxylation of the Centrosomal Protein Cep192.” *Developmental Cell* 26, no. 4 (August 2013): 381–92. doi:10.1016/j.devcel.2013.06.014.

Papandreou, I, Cairns, R A., Fontana, L., Lim, A L., and Denko, N C. “HIF-1 Mediates Adaptation to Hypoxia by Actively Downregulating Mitochondrial Oxygen Consumption.” *Cell Metabolism* 3, no. 3 (March 2006): 187–97. doi:10.1016/j.cmet.2006.01.012.

Schagger, H., and Pfeiffer, K. “Supercomplexes in the Respiratory Chains of Yeast and Mammalian Mitochondria.” *The EMBO Journal* 19, no. 8 (April 17, 2000): 1777–83. doi:10.1093/emboj/19.8.1777.

Schneider, M, Geyte, K V., Fraisl, P., Kiss, J., Aragonés, J., Mazzone, M., Mairbäurl, Het al. “Loss or Silencing of the PHD1 Prolyl Hydroxylase Protects Livers of Mice against Ischemia/reperfusion Injury.” *Gastroenterology* 138, no. 3 (March 2010): 1143–1154.e1–2. doi:10.1053/j.gastro.2009.09.057.

Schneider, C A., Rasband, W S., and Eliceiri, K W.,. “NIH Image to ImageJ: 25 Years of Image Analysis.” *Nature Methods* 9, no. 7 (July 2012): 671–75. doi:10.1038/nmeth.2089.

Scortegagna, M., Ding, K., Oktay, Y., Gaur, A., Thurmond, F., Yan, L-J., Marck, B T., et al. “Multiple Organ Pathology, Metabolic Abnormalities and Impaired Homeostasis of Reactive Oxygen Species in *Epas1*$^{-/-}$ Mice.” *Nature Genetics* 35, no. 4 (December 2003): 331–40. doi:10.1038/ng1266.

Seth, P., Krop, I., Porter, D., and Polyak, K. “Novel Estrogen and Tamoxifen Induced Genes Identified by SAGE (Serial Analysis of Gene Expression).” *Oncogene* 21, no. 5 (January 24, 2002): 836–43. doi:10.1038/sj.onc.1205113.

Shigenaga, M. K., Hagen, T. M., and Ames, B. N. “Oxidative Damage and Mitochondrial Decay in Aging.” *Proceedings of the National Academy of Sciences* 91, no. 23 (November 8, 1994): 10771–78.

Smith, A. C., Blackshaw, J. A., and Robinson, A. J., “MitoMiner: A Data Warehouse for Mitochondrial Proteomics Data.” *Nucleic Acids Research* 40, no. D1 (January 1, 2012): D1160–D1167. doi:10.1093/nar/gkr1101.

Takeda, K., Ho, V C., Takeda, H., Duan, L-J., Nagy, A., and Fong, G-H. “Placental but Not Heart Defects Are Associated with Elevated Hypoxia-Inducible Factor α Levels in Mice Lacking Prolyl Hydroxylase Domain Protein 2.” *Molecular and Cellular Biology* 26, no. 22 (November 2006): 8336–46. doi:10.1128/MCB.00425-06.

Wei, Y-H, Wu, S-B., Ma, Y-S., and Lee, H-C. “Respiratory Function Decline and DNA Mutation in Mitochondria, Oxidative Stress and Altered Gene Expression during Aging.” *Chang Gung Medical Journal* 32, no. 2 (April 2009): 113–32.

Wittig, I., Karas, M., and Schägger, H. “High Resolution Clear Native Electrophoresis for In-Gel Functional Assays and Fluorescence Studies of Membrane Protein Complexes.” *Molecular & Cellular Proteomics* 6, no. 7 (July 1, 2007): 1215–25. doi:10.1074/mcp.M700076-MCP200.

Zhang, Q., Gu, J., Li, L., Liu, J., Luo, B., Cheung, H-W., Boehm, J S., et al. “Control of Cyclin D1 and Breast Tumorigenesis by the EglN2 Prolyl Hydroxylase.” *Cancer Cell* 16, no. 5 (November 6, 2009): 413–24. doi:10.1016/j.ccr.2009.09.029.